

Review

Surface-Rupturing Historical Earthquakes in Australia and Their Environmental Effects: New Insights from Re-Analyses of Observational Data

Tamarah R. King ^{1,*} , Mark Quigley ¹ and Dan Clark ²

¹ School of Earth Sciences, University of Melbourne, Melbourne 3010, Australia; Mark.quigley@unimelb.edu.au

² Geoscience Australia, Canberra 2609, Australia; Dan.clark@ga.gov.au

* Correspondence: tamarah.king@unimelb.edu.au

Received: 2 August 2019; Accepted: 16 September 2019; Published: 20 September 2019;
Corrected: 10 February 2022



Abstract: We digitize surface rupture maps and compile observational data from 67 publications on ten of eleven historical, surface-rupturing earthquakes in Australia in order to analyze the prevailing characteristics of surface ruptures and other environmental effects in this crystalline basement-dominated intraplate environment. The studied earthquakes occurred between 1968 and 2018, and range in moment magnitude (M_w) from 4.7 to 6.6. All earthquakes involved co-seismic reverse faulting (with varying amounts of strike-slip) on single or multiple (1–6) discrete faults of ≥ 1 km length that are distinguished by orientation and kinematic criteria. Nine of ten earthquakes have surface-rupturing fault orientations that align with prevailing linear anomalies in geophysical (gravity and magnetic) data and bedrock structure (foliations and/or quartz veins and/or intrusive boundaries and/or pre-existing faults), indicating strong control of inherited crustal structure on contemporary faulting. Rupture kinematics are consistent with horizontal shortening driven by regional trajectories of horizontal compressive stress. The lack of precision in seismological data prohibits the assessment of whether surface ruptures project to hypocentral locations via contiguous, planar principal slip zones or whether rupture segmentation occurs between seismogenic depths and the surface. Rupture centroids of 1–4 km in depth indicate predominantly shallow seismic moment release. No studied earthquakes have unambiguous geological evidence for preceding surface-rupturing earthquakes on the same faults and five earthquakes contain evidence of absence of preceding ruptures since the late Pleistocene, collectively highlighting the challenge of using mapped active faults to predict future seismic hazards. Estimated maximum fault slip rates are 0.2–9.1 m Myr⁻¹ with at least one order of uncertainty. New estimates for rupture length, fault dip, and coseismic net slip can be used to improve future iterations of earthquake magnitude—source size—displacement scaling equations. Observed environmental effects include primary surface rupture, secondary fracture/cracks, fissures, rock falls, ground-water anomalies, vegetation damage, sand-blows/liquefaction, displaced rock fragments, and holes from collapsible soil failure, at maximum estimated epicentral distances ranging from 0 to ~250 km. ESI-07 intensity-scale estimates range by ± 3 classes in each earthquake, depending on the effect considered. Comparing M_w -ESI relationships across geologically diverse environments is a fruitful avenue for future research.

Keywords: Intraplate earthquake; surface rupture; Australian earthquakes; earthquake environmental effects; reverse earthquake; ESI 2007 scale; historical and recent earthquakes

1. Introduction

In the 50 years between 1968 and 2018 Australia experienced eleven known surface rupturing earthquakes (Table 1, Figure 1). Studies of Australian surface rupturing earthquakes have contributed

to improvements in our collective understanding of intraplate earthquake behavior, including rupture recurrence, in stable continental regions (SCR) [1–5] and empirically-derived scaling relationships for reverse earthquakes [6–9]. This paper reviews available published literature on historic surface ruptures (Tables 1 and 2) and collates geological data (Tables 3 and 4, Figures 1 and 2), seismological data and analyses (Table 5), surface rupture measurements (Table 6), environmental damage (Table 7), and paleoseismic data (Table 8) (Figures 3–10). We re-evaluate and reconsider rupture and fault characteristics in light of new data (e.g., geophysical and geological) using modern analysis techniques (e.g., environmental seismic intensity scale (ESI-07) [10]) and new or updated concepts in earthquake science since the time of publication (e.g., paleoseismology, SCR earthquake recurrence).

Table 1. Summary of known historic Australian surface rupturing earthquakes and relevant references.

Name	Fig. 1	Magnitude (Mw) [11]	Date (UTC)	This Paper:			Published		Relevant References
				Length (km)	Dip	Avg. Net-Slip (m)	Length (km)	Max. Vert. Disp. (m)	
Meckering, WA	1	6.59	14/10/1968	40 ± 5	35° ± 10	1.78	37	2.5	[12–37]
Calingiri, WA	8	5.03	10/03/1970	3.3 ± 0.2	20° ± 10	0.46	3.3	0.4	[23–25,38,39]
Cadoux, WA	4	6.1	02/06/1979	20 ± 5	60° ± 30	0.45	14	1.4	[28,40–45]
Marryat Creek, SA	5	5.7	30/03/1986	13 ± 1	40° ± 10	0.31	13	0.9	[1,28,46–49]
Tennant Creek 1 (Kunayungku) NT	7	6.27	22/01/1988	9 ± 1	40° ± 5	0.55	10.2	0.9	[1,49–69]
Tennant Creek 2 (Lake Surprise west)	6	6.44	22/01/1988	9 ± 2	60° ± 10	0.84	6.7	1.1	[1,49–69]
Tennant Creek 3 (Lake Surprise east)	3	6.58	22/01/1988	16 ± 0.5	35° ± 5	1.23	16	1.8	[1,49–69]
Katanning, WA	10	4.7	10/10/2007	0.5 ± 0.5	40° ± 5	0.2	1.26	0.1	[70,71]
Pukatja, SA	9	5.18	23/03/2012	1.3 ± 0.3	30° ± 10	0.25	1.6	0.5	[9,72]
Petermann, NT	2	6.1	20/05/2016	21 ± 0.5	30° ± 5	0.42	20	1.0	[73–78]
Lake Muir, WA		5.3	16/09/2018				3	0.5	[79]

Other literature with relevant analysis or data regarding historic ruptures: [80–98].

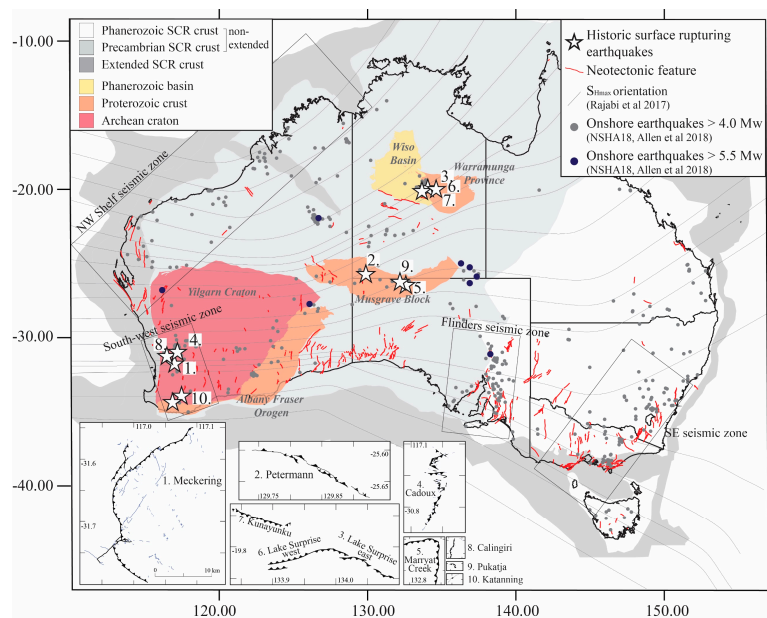


Figure 1. Map of Australia showing locations of historic surface rupturing events, continental scale crustal divisions [99], onshore historic seismology >4.0 (1840–2017) [11], simplified crustal stress trajectory map [100], GA neotectonic features database [95], recognized seismic zones [101,102] and specific crustal provinces relevant for surface rupture events (Table 3) [103]. Small maps show individual surface ruptures at the same scale and ordered by rupture length (excluding 2018 Lake Muir).

Australia is regarded as a stable continental region [104] surrounded by passive margins with an intraplate stress field controlled by plate boundary forces [100,105] (Figure 1). This stress field has been extant throughout much of Australia since the late Miocene, broadly concurrent with a rearrangement of tectonic boundaries in India, New Zealand, New Guinea, and Timor [101]. More than 360 potentially neotectonic features (those showing displacements associated with, or since initiation of, the current stress-field conditions) [5,95] have been recognized in the landscape through field mapping, subsurface geophysical imaging, digital elevation modelling, and palaeoseismic investigation [2,3,5,34,95,106–113] (Figure 1).

Southeast Australia and the Flinders Ranges (Figure 1) have the highest rates of seismicity [101,102] and estimated neotectonic fault slip rates [3,109,111] yet all of the largest onshore historic Australian earthquakes have occurred in Archean to Proterozoic cratonic crust across the central and western parts of the country (Figure 1) [11]. Of four defined zones of high seismicity (Figure 1) [101,102], the South West Seismic Zone (SWSZ) is the only to coincide with historic surface ruptures (Meckering, Calingiri, Cadoux, Katanning, Lake Muir). Other ruptures (Marryat Creek, Tennant Creek, Pukatja, Petermann) have occurred in historically aseismic regions of the cratonic crust (Figure 1, Table 5, Section 3.2).

Table 2. Summary of data sources used in reviewing Australian historic surface ruptures.

Seismological Catalogues	
Primary literature	[9,12,15,18,24,25,38,40,41,43,46,47,57,60,61,63,70,73–75,88]
Geoscience Australia (GA) online catalogue	https://earthquakes.ga.gov.au/
National Seismic Hazard Assessment 2018 (NSHA18)	http://pid.geoscience.gov.au/dataset/ga/123139/ ; [11]
Focal Mechanisms	
Primary literature	[9,23,26,28,41,43,46,55,57,60,70,73,74]
GA compilation	[90]
Global centroid moment tensor catalogue	https://www.globalcmt.org/CMTsearch.html
Surface Rupture Trace	
Primary literature	[9,25,41,48,63,70,73,78]
GA Neotectonic Features Database	[95]; http://pid.geoscience.gov.au/dataset/ga/74056
Google satellite imagery	https://www.google.com/earth/
Bing satellite imagery	https://www.bing.com/maps/aerial
National SRTM DEM	SRTM 1-Sec DEM: http://pid.geoscience.gov.au/dataset/ga/72759
Geological Maps	
Primary literature	[9,16,25,41,65,114–117]
Geological Survey of Western Australia	http://www.dmp.wa.gov.au/Geological-Survey/Geological-Survey-262.aspx
Northern Territory Geological Survey	https://geoscience.nt.gov.au/
Geological Survey of South Australia	http://www.energymining.sa.gov.au/minerals/geoscience/geological_survey
Geoscience Australia	https://ecat.ga.gov.au/geonetwork/srv/eng/catalog.search
Borehole Data	
Northern Territory Government	http://nrmaps.nt.gov.au/nrmaps.html
South Australia Government	https://www.waterconnect.sa.gov.au/Systems/GD/Pages/Default.aspx
Geophysical Maps	
Primary literature	[33,50,51]
Bouguer gravity anomaly	http://pid.geoscience.gov.au/dataset/ga/101104
Total magnetic intensity	http://pid.geoscience.gov.au/dataset/ga/89596
Rupture Offset Data	
Primary literature	[9,25,41,48,62,63,70,73,77]
Historic Photos of Ruptures	
Primary literature	[1,9,12,14,15,25,35,37,40,41,47,48,59,63,64,72,73,87,118]
Websites	https://aees.org.au/
News articles	http://fortennantcreekers.com/events/earthquake-friday-22-january-1988/ https://trove.nla.gov.au/ ; https://www.abc.net.au/news/

2. Review Data, Methods and Terminology

Publications reviewed for ten of the eleven historic ruptures are provided in Table 1. At the time of writing, no publications are available for the most recent (eleventh) earthquake (8 November 2018 Mw 5.3 Lake Muir earthquake), although one is currently in review [79] and some imagery and data are available online (<https://riskfrontiers.com/the-2018-lake-muir-earthquakes/>, <https://www.abc.net.au/news/2018-11-09/earthquake-hits-lake-muir-western-australia/10480694> (accessed on 21 June 2019)). Available details for this event are included in Tables 1, 3 and 7 but it is otherwise not investigated in this paper. The Tennant Creek event comprises three mainshocks in a 12-hr period on the 22 January 1988, with three separate scarps recognized at the surface. Analysis of available seismological and

surface data supports a direct association between each mainshock and an individual rupture (TC1: Kunayungku; TC2: Lake Surprise west; TC3: Lake Surprise east) [57,59,62,69] and they are treated as separate events in this paper.

Relevant papers were identified by reading through either (a) reference lists of recent (2010–2018) publications or (b) the citation history of older publications using Google Scholar. In total $N = 67$ articles were identified as containing relevant primary data and interpretations for individual or multiple surface rupturing events (Table 1). A further 16 publications were identified containing relevant information on Australian seismicity (drawing on data from the primary publications) or compilations of previously published material (Table 1). Other sources of data used to complement analysis of primary published data are summarized in Table 2.

Epicenter locations and focal mechanisms were collated from primary literature and online databases (Table 2). Geoscience Australia (GA) maintain an online earthquake catalogue that is continuously updated and recently published a national earthquake catalogue (NSHA18) from 1840 to 2017 [11]. The NSHA18 catalogue contains revised magnitude values (M_w) for all surface rupturing events based on a comprehensive reanalysis [11,119], which are used in this study. Epicenters for surface rupturing events are generally located closer to the surface ruptures in the online database than the NSHA18 catalogue.

Published surface rupture maps were previously digitized into GA's publicly available Neotectonic Features Database [95]. In this paper, we sourced the original maps, georeferenced them, and digitized secondary fracturing that was left out of the GA database (Figures 3–10). Some ruptures were relocated up to 200 m from the locations in the Neotectonic Features Database based on infrastructure and visible surface rupture matched on high resolution satellite imagery (Table 2) and primary maps, to correct for datum transformation errors.

For the purposes of this paper we use the terms “surface rupture” and “scarp” to describe the primary zone along which hanging-wall and foot-wall offset is visible at the surface. Fracturing relates to secondary surface features which do not host significant displacement, associated with the primary rupture (e.g., cracking). “Fissures” describe significant extensional cracks often with non-seismic edge collapse extending their width. “Fault” is used to describe the seismologically defined plane of rupture, of which the surface rupture is the observable expression.

3. Results

Detailed summaries of the geology, seismology, surface rupture and palaeoseismology for the eleven considered historical surface ruptures from 1968 to 2016 are available as seven EarthArXiv reports ([120–126]). Figures and data in these reports include available geological maps, geophysical maps, borehole data, surface rupture maps, displacement data, and available palaeoseismic trench logs. In the process of reviewing available literature, a number of inconsistencies in data usage or reproduction were identified. These are summarized in Section 4.1 of this paper, with more detail available in the EarthArXiv reports. Below is a concise summary of the seven reports (the three Tennant Creek ruptures are contained within a single report) with key data presented in Tables 3–9 and Figures 3–10, and provided as Supplementary Data.

3.1. Geology

The Meckering, Calingiri, Cadoux, and Katanning events occurred in the Archean Yilgarn Craton within ~25 km of significant terrane boundaries (Figure 1). The Lake Muir event occurred in the Albany-Fraser Orogen, <15 km south of the south dipping terrane boundary with the Yilgarn Craton (Figure 1). The Marryat Creek, Pukatja and Petermann events occurred within the Mesoproterozoic Musgrave Block (Figure 1) within 0–10 km of major terrane boundaries. The Tennant Creek ruptures extend across the boundary of the Proterozoic Warramunga Province and Neoproterozoic–Cambrian Wiso Basin (Figure 1) (summary of all regional geology in Table 3, comprehensive details in EarthArXiv reports [120–126]).

Table 3. Summary of regional geology for each historic surface rupture.

Rupture	Refs.	Geological Province			Nearby Regional Structure				
		Name	Age	Sub-Division	Name	Age	Geometry	Dist. from Rupture	Approx. Aligned?
Meckering	[33,91,108,127]	Yilgarn Craton	Archean	Jimperding Metamorphic Belt, Lake Grace Terrane	Boundary Lake Grace and Boddington Terranes	Archean	NW-SE, shallow E dipping suture	~25 km on HW	Yes
Calingiri	[91,108,127]	Yilgarn Craton	Archean	Jimperding Metamorphic Belt, Lake Grace Terrane	Boundary Lake Grace and Boddington Terranes	Precambrian	NW-SE, shallow E dipping suture	~10 km on HW	Yes
Cadoux	[91,108,127]	Yilgarn Craton	Archean	Archean greenstone	Boundary Murchison Terrane and Southern Cross Province	Archean	N-S	~10 km?	Yes
Marryat Creek	[128–131]	Musgrave Block	Mesoproterozoic	Fregon Domain	Mann Fault	Neoproterozoic	ENE-WSW, ~1km wide suture	<0.5 km	Yes (part)
Kunayungku ^	[66,68]	Wiso Basin	Neoproterozoic – Cambrian	–	–	–	–	–	–
Lake Surprise west ^	[66,68]	Tennant Creek Region	Paleoproterozoic	Warramunga Province	–	–	–	–	–
Lake Surprise east ^	[66,68]	Tennant Creek Region	Paleoproterozoic	Warramunga Province	–	–	–	–	–
Katanning,	[91,108,127]	Yilgarn Craton	Archean	Boddington Terrane	–	–	–	–	–
Pukatja	[128–131]	Musgrave Block	Mesoproterozoic	Fregon Domain	Woodroffe Thrust	Neoproterozoic	NE-SW, ~30° S, ~3 km wide suture	~10 km on HW	No
Petermann	[116,128–131]	Musgrave Block	Mesoproterozoic	Fregon Domain	Woodroffe Thrust	Neoproterozoic	NW-SE, ~30° S, ~3 km wide suture	~ 10 km on HW	Yes
Lake Muir		Albany Fraser Orogen	Proterozoic	Biranup Zone	Boundary Yilgarn and Albany Fraser Orogen	Mesoproterozoic	E-W, S dipping, ~10–20 km wide shear zone	~ 5–15 km on HW	No

^ Tennant Creek scarp.

Granitic gneiss, migmatite, mylonite, granulite, and/or amphibolite basement rock is observed in trenches or outcrop at <1 m depth at multiple locations along the Petermann (Figure 2), Pukatja, Marryat Creek (Figure 2), Cadoux and Meckering ruptures. Proterozoic basement in the vicinity of the Tennant Creek ruptures is variably overlain by 10 s to 100 s of meters of Phanerozoic basin bedrock. Structural measurements (foliations, intrusive boundaries) for bedrock outcrops within 5 km of surface ruptures are qualitatively well-aligned to surface ruptures in eight of ten events, though dip measurements are only qualitatively well aligned in three cases. This may relate to dip measurement difficulties for heavily weathered bedrock. (Summary of basement/bedrock in Table 4, comprehensive details in EarthArXiv reports [120–126]).

Nine of ten ruptures align with linear magnetic anomalies (Figure 2) and six align with linear gravity anomalies/gradients. The Katanning rupture does not align with either gravity or magnetics at the scale of available geophysical data (Figure 2, Table 2), and the Lake Muir rupture was not studied in this paper (paper in review: [79]). In cases where surface rupture traces are highly curved, arcuate, and/or segmented (Meckering, Marryat Creek, Tennant Creek, Pukatja), the distinctly-oriented rupture traces all align with distinct orientations of linear geophysical anomalies interpreted as faults, dikes, and lithological contacts (e.g., [33]).

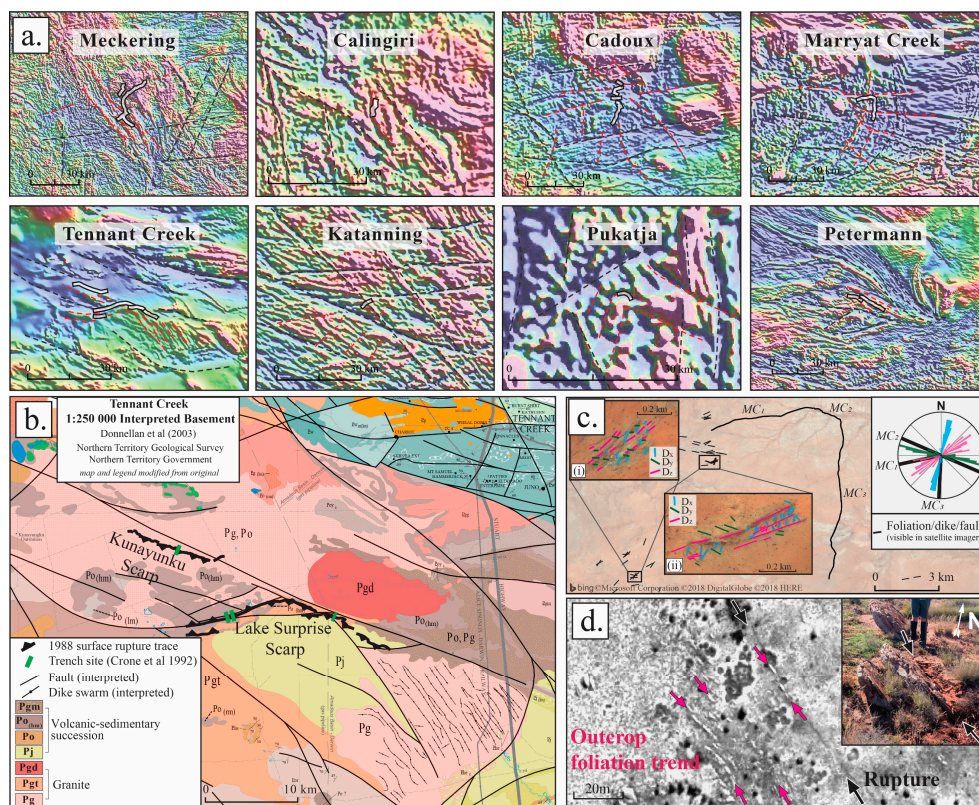


Figure 2. Examples of the relationship between geophysical data and surface outcrop to historic ruptures (a) national total magnetic intensity map with ruptures overlaid, and dashed lines indicating linear anomalies (b) interpreted basement geology around the three Tennant Creek scarp (no basement outcrops at the surface) demonstrating strong correlation between intrusive/lithological boundaries, basement faults, and historic surface rupture (legend heavily simplified to show lithologies around the ruptures, more details in EarthArXiv report [126] legend and original map. Map used under creative commons NT Gov) (c) examples of surface outcrop structures visible in basement around the Marryat Creek rupture including three sets of dike/foliation/fault orientations coincident with the three major orientations of the historic rupture, uninterpreted satellite imagery insets (i) and (ii) available in Marryat Creek EarthArXiv report [123] (d) example of mylonite foliation orientation along a section of the Petermann rupture where outcrop occurs within the primary rupture zone.

Table 4. Degree of alignment between rupture, basement structures, and geophysical anomalies.

Rupture	Refs.	Mapped Basement							Geophysics				Evidence of Basement Control on Rupture	
		Description	Depth (m)	Method *	Dominant Strikes	Alignment	Dips	Alignment	Mag.	Alignment	Gravity	Alignment	Y/N	Type #
Meckering	[16,25,33,114]	Granites, gneiss, mafic dikes	0–20	Geol.	NW, SW	Mod.	55°–90°	Low	Yes	Very high	Part	Mod.	Y ¹	FL _{CS} , V _S , D _G , FD _{CS}
Calingiri	[25,114]	Migmatite, gneiss	0–20	Geol.	NE	High	60°–90°	Low	Yes	High	Yes	High	Y	FL/FD _G
Cadoux	[41,115]	Granite, gneiss, mafic dikes	0–20	Geol. + BH	N, NW, NE, W	High	50°–90°	Mod.–High	Yes	Very high	Yes	Mod.	Y ²	FL _{CS} , V _S , D _G
Marryat Creek	[47,48,117]	Mylonite, gneiss, granite, mafic dikes	0–5	Geol. + BH	W, NNE, NE	Very high	–	–	Yes	Very high	Part	High	Y ³	FL _{CS} , FT _{CS} , D _{CS}
Kunayungku ^	[50–52,66,68,132]	Schist, granite	50+	BH + Geo.Int.	NE	Very high	–	–	Yes	High	Yes	Very high	Y ⁴	FT _G
Lake Surprise west ^	[50,51,66,68,132]	Metavolc., metased., granite	220+	BH + Geo.Int.	NW	Very high	–	–	Yes	Very high	No	–	Y ⁵	FT _G , L _G
Lake Surprise east ^	[50,51,66,68,132]	Metavolc., metased., granite	50+	BH + Geo.Int.	NE	Very high	–	–	Yes	Very high	Yes	High	Y	FT _G , L _G
Katanning,	[133]	Granite, gneiss	–	Geol.	NW	Very low	–	–	No	–	No	–	N	–
Pukatja	[9]	Granite, gneiss	0–10	Geol.	NE	High	30°	Very high	Yes	Very high	No	–	Y ⁶	L _{CS} , FL _{CS}
Petermann	[73,128,134]	Mylonite	0–10	Geol. + BH	NW	Very high	20°–50°	Very high	Yes	Very high	Yes	Very high	Y ⁷	FL _{CS}

^ Tennant Creek scarp. * 1:250,000 surface geology map (Geol.), ground-water borehole records (BH), geophysical interpretation (Geo.Int.). # Evidence for basement control: foliation (FL); fault (FT); fold (FD); vein (V); dike (D); lithological/batholith (L); geophysical (C)/surface (S) with specific examples detailed below: ¹ Rupture along brecciated quartz in cutting / trench [25]. ² Tank scarp ruptures through surface granite, and along a quartz vein in a hand-dug trench; bedrock within 10 m of the Kalajzic scarp aligned with rupture [41]. ³ Two trenches confirm rupture occurred along a pre-existing Proterozoic fault [118]. ⁴ Normal fault interpreted below Kunayungku scarp from ground-water boreholes and geophysical data prior to rupture (1981) [52,59]. ⁵ Lake Surprise west scarp runs along a 1–2 m high quartz ridge, associated with fluid movement along a bedrock fault [59,63,64]. Bedrock does not outcrop at the surface. ⁶ Rupture aligns with the projected boundary between a granite batholith and granulite facies gneiss; rupture curves around outcrop of granite batholith [9]. ⁷ Rupture abuts mylonite outcrop with the same strike and dip; mylonite with the same strike and dip outcrops within 1 m of the scarp in multiple locations [73].

3.2. Seismology

The sparse nature of the Australian National Seismograph Network (<https://www.fdsn.org/networks/detail/AU/>) results in large (i.e., ≥ 5 –10 km) uncertainties in earthquake epicenter and hypocenter location estimates that are difficult to quantify, including those for the earthquakes studied here [102]. Epicentral determinations (Figures 3–10) are typically not sufficiently accurate to unambiguously associate with surface ruptures. Six of ten ruptures have favored epicenter locations that are located on the rupture hanging-wall, within approximated positional uncertainty bounds.

Many publications do not state statistical uncertainties for their epicenter locations. Uncertainties listed in Table 5 include published uncertainties or an assigned value of ± 10 km where no uncertainties are available [102]. Epicenters with lower uncertainties are derived using a variety of relocation methods including extra analysis (e.g., InSAR slip distributions, joint hypocenter determination) or extra data (e.g., surface rupture location, aftershocks from temporary seismometer arrays) (comprehensive details in EarthArXiv reports [120–126]). The epistemic uncertainty relating to the quality of velocity models used to locate epicenters is unconstrained but appears to be one of the major sources of inaccurate locations where instrumentation is particularly sparse. For instance, epicenters for Pukatja and Marryat Creek are located up to 17 and 30 km from the identified surface rupture respectively, showing large uncertainties still affecting remote earthquake locations between 1986–2012.

Hypocenters derived from mainshock instrumental data do not project onto rupture planes as defined by surface rupture for any of the studied events. Hypocentral depth estimates based on aftershock data and relocated epicenter locations suggest depths of < 5 km (for Tennant Creek [59], Petermann [73] and Meckering [37]). Centroid moment tensor depths are < 6 km depth, with the authors' preferred best-fits all < 4 km depth (Meckering [26–28]; Cadoux [28]; Marryat Creek [28]; Tennant Creek [55]; Katanning [70]; Petermann [74]).

Epicentral location uncertainties limit the study of rupture propagation direction(s) for most events. Model scenarios for the Meckering earthquake support a bilateral rupture [37]. Unilateral upwards propagation has been proposed for the first Tennant Creek mainshock, complex propagation in the second mainshock, and unilateral upwards propagation to the Southeast in the third mainshock (all on separate faults) [57].

Seven of ten events show foreshock activity within six months and 50 km of the mainshock epicenter and six of ten show instrumentally recorded prior seismicity (more than five events within 10 years and 50 km). Precise locations are difficult to obtain due to epistemic and statistical uncertainties, particularly for assessing seismicity prior to 1980 due to sparse instrumentation [102]. Aftershock data are inherently incomplete for most events due to sparse instrumentation. However, temporary seismometers were deployed following most events and magnitude completeness from the national network is > 3.0 Mw for all events [102] (though, the locations of these events are generally highly uncertain compared to the temporary arrays, as discussed above). The Musgrave block events (Marryat Creek, Pukatja, Petermann, Figure 1, Table 3) show less aftershock activity in comparison to the Tennant Creek and Western Australia earthquakes (Meckering, Calingiri, Cadoux) which had extended aftershock sequences [5,34].

Table 5. Summary of seismological data and interpretations for each rupture.

Rupture	Refs.	Published Epicenters		Located on Hanging-Wall		Hypocenter Depth ¹ (km)		Focal Mechanisms			Rup. Propagation	Foreshocks ⁴	Prior Seismicity ⁵	
		N=	Uncert. ² (km)	Initial	Relocated	Range	Uncert.	N=	CMT Depth ³ (km)	Dip Range				Strike Corr. with Rupture?
Meckering	[11,12,15,18,23–26,28,90]	8	~10	1	2	2.5–13	1–10 km	4	1.5–3	29°–45°	Yes	Bilateral	Yes	Yes
Calingiri	[11,23,25,38]	2	~10	0	1	1–15	>5	1		50°	Yes	Unknown	Yes	Yes
Cadoux	[11,28,40,41,43]	6	~10	N/A ⁶	N/A ⁶	3–15	>5	4	4–6	N/A ⁶	Part ⁶	Unknown	Yes	Yes
Marryat Creek	[11,28,46,47,88]	7	>10	0	1	5–19	>5	3	0–3	35°–67°	Part	Unknown	No	No
Kunayungku [^]	[11,55,57,60,61,63]	4	2–10	?	0	5–6.5	1–4	4	2.7	35°–55°	Yes	Unilateral	Yes	Yes
Lake Surprise west [^]	[11,55,57,60,61,63]	4	2–10	?	2	3–4	0.5–3	4	3.0	38°–70°	Part ⁷	Unknown	Yes	Yes
Lake Surprise east [^]	[11,55,57,60,61,63]	4	2–10	?	4	4.5–5	0.5–3	4	4.2	36°–45°	Yes	Unilateral	Yes	Yes
Katanning,	[70]	3	0.04–5	0	2	<1		1		43°	Yes	Unknown	No	No
Pukatja	[9,11]	6	>10	0	1	4–12	5?	3		45°–72°	Yes	Unknown	No	No
Petermann	[73–75]	6	2.5–8	4	2	1–10	>5	4	1–2	26°–52°	Yes	Unknown	yes	No

[^] Tennant Creek scarp. ¹ Includes both initial hypocentral depth estimates, and revised depths based on aftershock depths and locations, uncertainties from source literature. ² Epicenter uncertainty based on published uncertainties and/or estimate based on published uncertainties for similar events. ³ Centroid moment tensor depth, preferred value from publication. ⁴ Earthquake within 6 months and 50 km of epicenter (affected by catalogue completeness for very remote events, see EarthArXiv reports ([120–126]) for details). ⁵ Earthquakes (n > 5) within 10 years and 50 km of the epicenter (affected by catalogue completeness for very remote events, see EarthArXiv reports for details). ⁶ Geometry of the seismogenic fault is unclear as scarps in the Cadoux rupture dip both east and west. ⁷ Waveform analysis of the second Tennant Creek mainshock show complicated rupture, potentially related to complex fault interaction

3.3. Surface Ruptures

Methods for the original mapping of individual ruptures are summarized in Table 6 and give some indication of data quality (explored in more detail in EarthArXiv reports [120–126]). Some readjustment of terminology and classification is required when considering the earlier ruptures (e.g., ‘fault’ may refer to both primary rupture and secondary fractures) and considerable detail of rupture morphology was lost between fine-scale (i.e., 1:500) and whole rupture (1:25,000–1:50,000) for pre-digital maps (Meckering to Tennant Creek). Six of ten ruptures are concave relative to the hanging-wall, three are straight and one is slightly convex (Petermann) (Table 6). All ruptures are reverse, and only two events have surface measurements consistent with secondary lateral movement (Meckering: dextral; Calingiri: sinistral; Table 6, explored in individual EarthArXiv reports [120–126]).

Nine of ten ruptures studied (Katanning was excluded due to lack of field mapping) show a relationship between surface sediments/bedrock depth to rupture morphology. Discrete rupture and duplexing rupture are more common where bedrock is close to the surface or surface sediments are predominately calcrete/ferricrete/silcrete. Where sands dominate in the surface sediments, rupture tends to present as warping and folding, or correspond with breaks in visible surface rupture (e.g., Petermann: morphology explored in individual EarthArXiv report [125]).

Figures 3–10 show digitized versions of published primary ruptures, secondary fracturing, and dip values measured at the surface. Primary sources inconsistently derive published length values to describe their mapped rupture (Tables 1 and 6; explored in detail in EarthArXiv reports [120–126]) which are then used in secondary sources including scaling relationships. This includes simplifying scarps to straight lengths (Calingiri, Cadoux, Marryat Creek), capturing along-rupture complexity to varying degrees (Pukatja, Tennant Creek), excluding segments that have length, offset and morphology characteristics of primary rupture (Meckering, Tennant Creek, Cadoux), and reporting InSAR derived lengths rather than visible rupture (Katanning). (Explored in more detail in individual EarthArXiv reports [120–126]).

Measurements of rupture length in the past have been inconsistent in their approach. Here, we re-classify mapped primary ruptures from original primary sources in order to generate a consistent rupture length dataset (Table 6). We simplify ruptures to straight lines and define new faults where mapped primary rupture has gaps/steps > 1 km and/or where strike changes by $> 20^\circ$ for distances > 1 km [135]. The Splinter and Burges scarps (Meckering), Lake Surprise west foot-wall scarp (Tennant Creek), and individual Cadoux scarps were not included in original published lengths. These features show offsets, lengths, and locations consistent with primary slip along basement structures proximal to the main scarps, and therefore we include them in our length values.

Where InSAR is available (Katanning and Petermann) we present fault lengths described by both visible rupture and InSAR (Table 6). Visible rupture in the Petermann event was highly segmented due to ineffective rupture propagation through sand dunes up to six metres high [73]. Due to this we apply a slightly altered set of criteria to this event, faults are defined where strike of visible rupture and InSAR changes by $> 20^\circ$ and/or where steps in InSAR and visible rupture are > 1 km (Figure 10) [75,78].

Under these criteria seven of ten ruptures have more than one source fault defined (i.e., a multi-fault rupture). The total length of faulting is the same as published values for two events, increases by 2%–51% for four events relative to published length, and decreases by 4%–60% for three events (Tables 1 and 6). These lengths describe primary surface ruptures in a consistent way, accounting for all segments of rupture which show evidence of slip along basement structures. Our preferred length for each rupture, including uncertainties, is presented in Tables 1 and 6.

Table 6. Summary of surface measurements for each rupture.

Rupture	Refs.	Method ³	Shape ⁴	Published		Simplified Faults ¹			Preferred:		Displacement ² (m)						Disp. Profile Shape ⁶	
				Length (km)	Kin.	Dip Range	N=	Sum Length (km)	% Diff. Publ.	Length (km)	Dip	Max Vert. Disp.	Avg. Vert. Disp. ⁵	% Diff.	Max Net Slip	Avg. Net Slip ⁵		% Diff.
Meckering (Splinter)	[25]	FW; A; S _B	CC	37	R(D)	15–54°	4	44.4	+20%	40 ± 5	35° ± 10	1.98	0.97	51%	3.7	1.78	52%	S. Tg.
Calingiri	[25]	FW	S	9	R	24–42°	3					0.67	0.22	67%	1.34	0.44	67%	AS. Tg.
Cadoux	[25]	FW	S	3.3	R(S)	12–31°	1	3.3	0%	3.3 ± 0.2	20° ± 10	0.38	0.15	61%	1.26	0.46	63%	AS. Tg.
Marryat Creek	[41]	FW; A; S _B	CC/S	14	R	20–80°	6	20.6	+47%	20 ± 5	60° ± 30	1.4	0.35	75%	1.79	0.45	75%	AS. Tg.
Kunayungku	[48]	FW; A; S _C	CC	13	R	36–60°	3	13.6	+4%	13 ± 1	40° ± 10	0.9	0.21	77%	1.07	0.31	71%	Avg.
Lake Surprise west (LS west foot-wall)	[63]	FW; A; S _C	S	10.2	R	58°	1	8.6	–15%	9 ± 1	40° ± 5	0.9	0.36	60%	1.41	0.55	61%	S. Tg.
Lake Surprise east	[63]	FW; A; S _C	CC	6.7	R	65–84°	1	10.1	+51%	9 ± 2	60° ± 10	1.13	0.45	60%	2.26	0.84	63%	AS. Sine
Katanning (visible) ⁷	[70, 71]		S	3.1	R		1					0.74	0.43	42%	1.16	0.9	22%	Avg.
Katanning (InSAR)	[63]	FW; A; S _C	CC	16	R	28–30°	2	15.3	–4%	16 ± 0.5	35° ± 5	1.8	0.61	66%	3.6	1.23	66%	Avg.
Pukatja	[70, 71]	In.		0.3	R		1	0.3	0%	0.5 ± 0.5	40° ± 5	0.1						
Petermann (visible)	[70]	In.		2.5 ⁸			1	2.2	–12%			0.2 ⁸	0.1	50%	0.32 *	0.2 *	38%	AS. Tg.
Petermann (InSAR)	[9]	FW	CC	1.6	R	22–28°	1	1.0	–60%	1.3 ± 0.3	30° ± 10	0.48	0.12	75%	0.96	0.25	74%	AS. Sine
	[73, 77]	FW; S _C ; In; D; SI	CV	20	R	25–36°	3	21	+5%	21 ± 0.5	30° ± 5	0.96	0.2		1.92	0.42	78%	Avg.
	[73]	In.		21			2	21.5	+2%									

¹ Where mapped primary rupture has a gap/step > 1 km and/or change in strike > 20° across a length > 1 km (except where InSAR is available to validate rupture continuing along strike across gaps > 1 km). Lengths of individual faults available in EarthArXiv reports [120–126]. ² Vertical and lateral displacements digitized from original publications. Net slip calculated for this study. ³ Original mapping method: Field work (FW); aerial photographs (A); surveying (levelling, cadastral or GPS) basic (S_B), comprehensive (S_C); InSAR (In); Drone (D); Satellite (SI). ⁴ Concave (CC) relative to hanging-wall, convex (CV) relative to hanging-wall, straight (minor deviations but overall straight shape). ⁵ Length weighted average across 0.5 km increments (where rupture length > 5 km) or 0.1 km increments (where rupture length < 5 km). ⁶ Profile shape based on Wesnousky (2008) [7] from visual fit (e.g., not best-fit regression curves): symmetrical (S); asymmetrical (AS); triangle (Tg); sine; average line (Avg). ⁷ Katanning visible surface rupture was observed, but no field mapping was conducted [70,71]. Original and subsequent publications describe Katanning length based on best-fit InSAR-derived source parameters (1.26 km) [70], rather than length of InSAR trace (2.5 km). Offset comes from field estimates (0.1 m) and fault modelling from InSAR data [70].

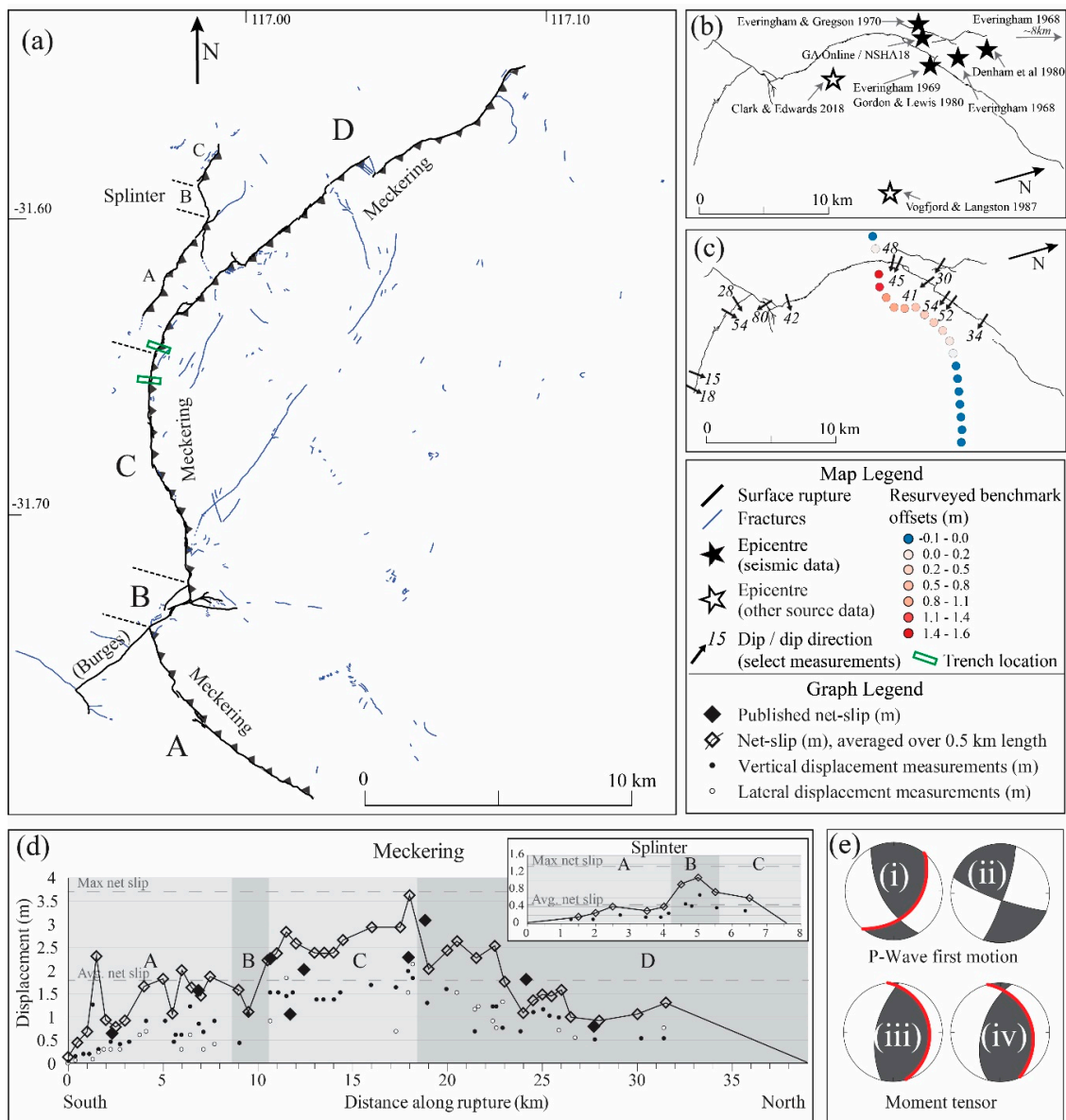


Figure 3. 1968 Mw 6.6 Meckering earthquake (a) rupture and fracture map of Meckering and Splinter scarps [25] with faults labelled as per displacement graphs, trench location from [37] (b) published epicenter locations, open stars show approximate locations of epicenters without published coordinates (c) selected dip measurements of scarp and displacement of resurveyed road benchmarks [25] (d) graphs of along-rupture vertical and lateral displacement measurements and net slip calculations [25] and net slip calculated from available data averaged over 0.5 km increments (this study) (e) focal mechanisms (red line shows preferred plane from original publication) from (i) Fitch et al., 1973, (ii) Fitch et al., 1993 & Leonard et al., 2002, (iii) Fredrich et al., 1988, and (iv) Vogtfjord and Langston 1987.

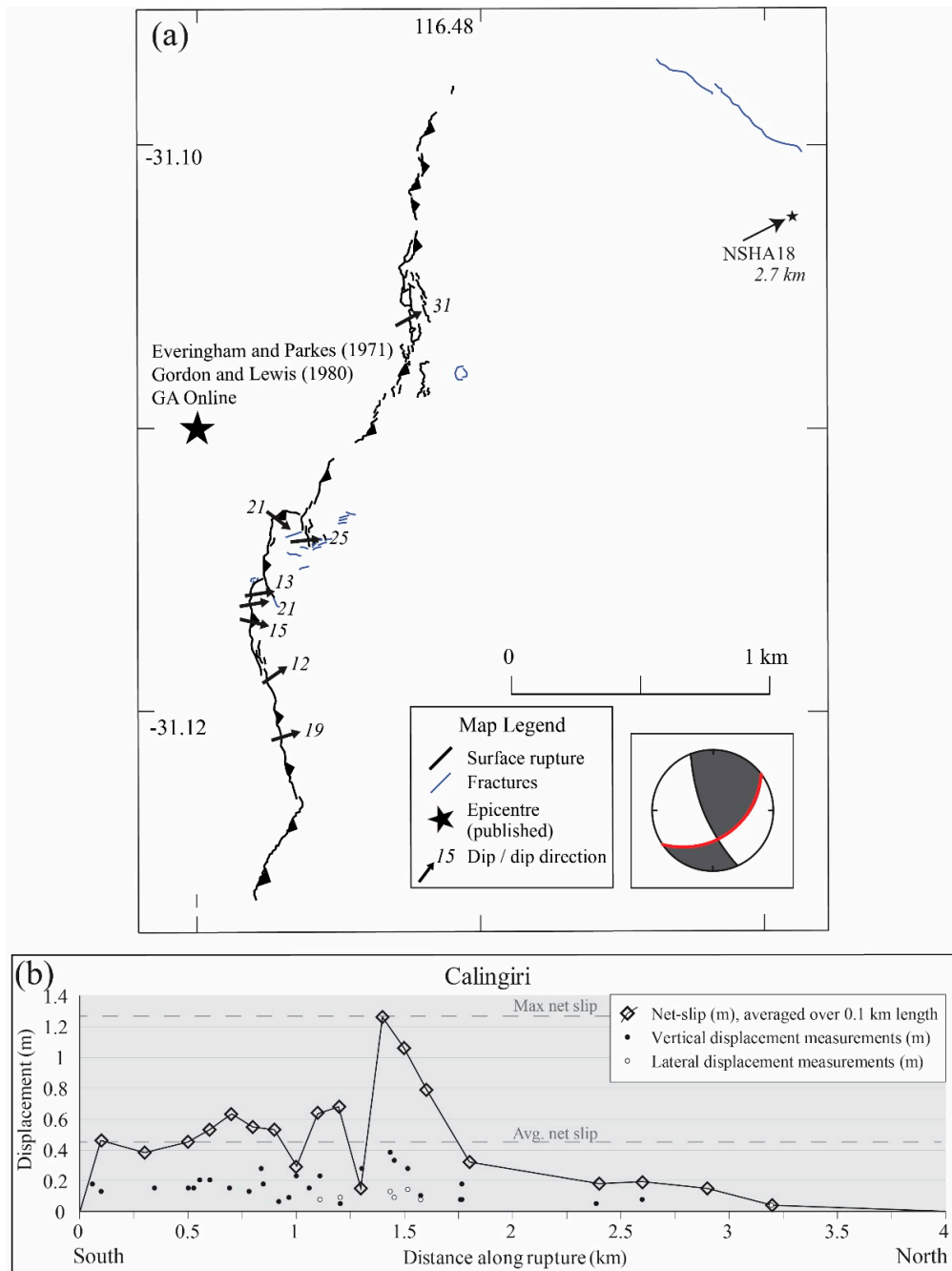


Figure 4. 1970 Mw 5.0 Calingiri earthquake (a) rupture and fracture map of Calingiri [25] showing published epicenter locations and dip measurements of scarp [25], focal mechanism (red line shows preferred plane from original publication) from Fitch et al., 1973 (b) graph of along-rupture vertical and lateral displacement measurements [25] and net slip calculated from available data averaged over 0.1 km increments (this study).

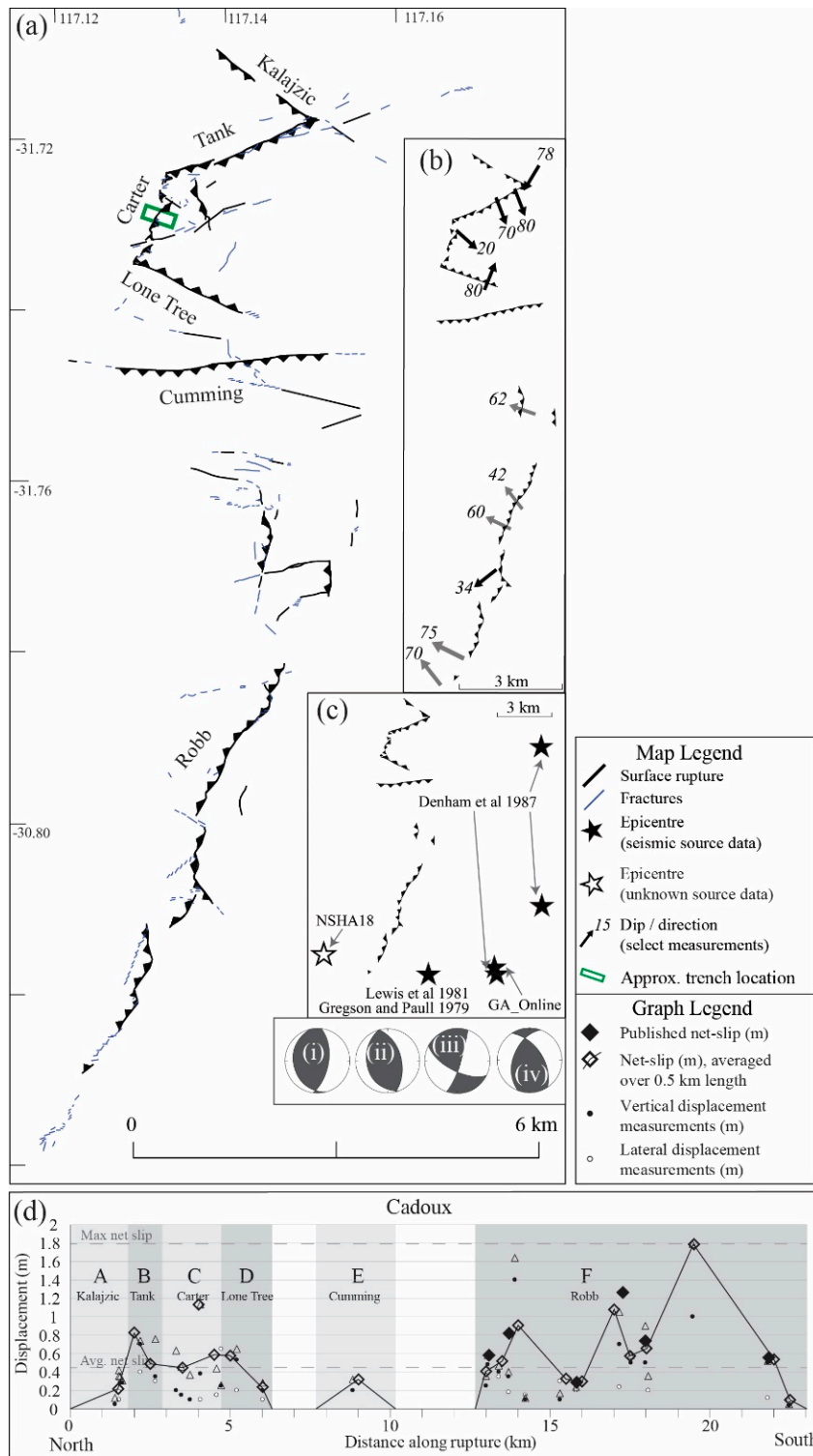


Figure 5. 1979 Mw 6.1 Cadoux earthquake (a) rupture scarps and fracturing involved in the Cadoux rupture with named faults [41], focal mechanisms from (i) Denham et al., 1987 (ii) Fredrich et al., 1988 (iii) Everingham and Smith (unpublished, Lewis et al., 1981) (iv) CMT (b) available dip measurements, black where directly measured and grey were calculated based on available displacement measurements [41] (c) published epicenter locations (d) graph along-rupture of vertical and lateral displacement measurements and calculated net slip [41] and net slip calculated from available data averaged over 0.5 km increments (this study).

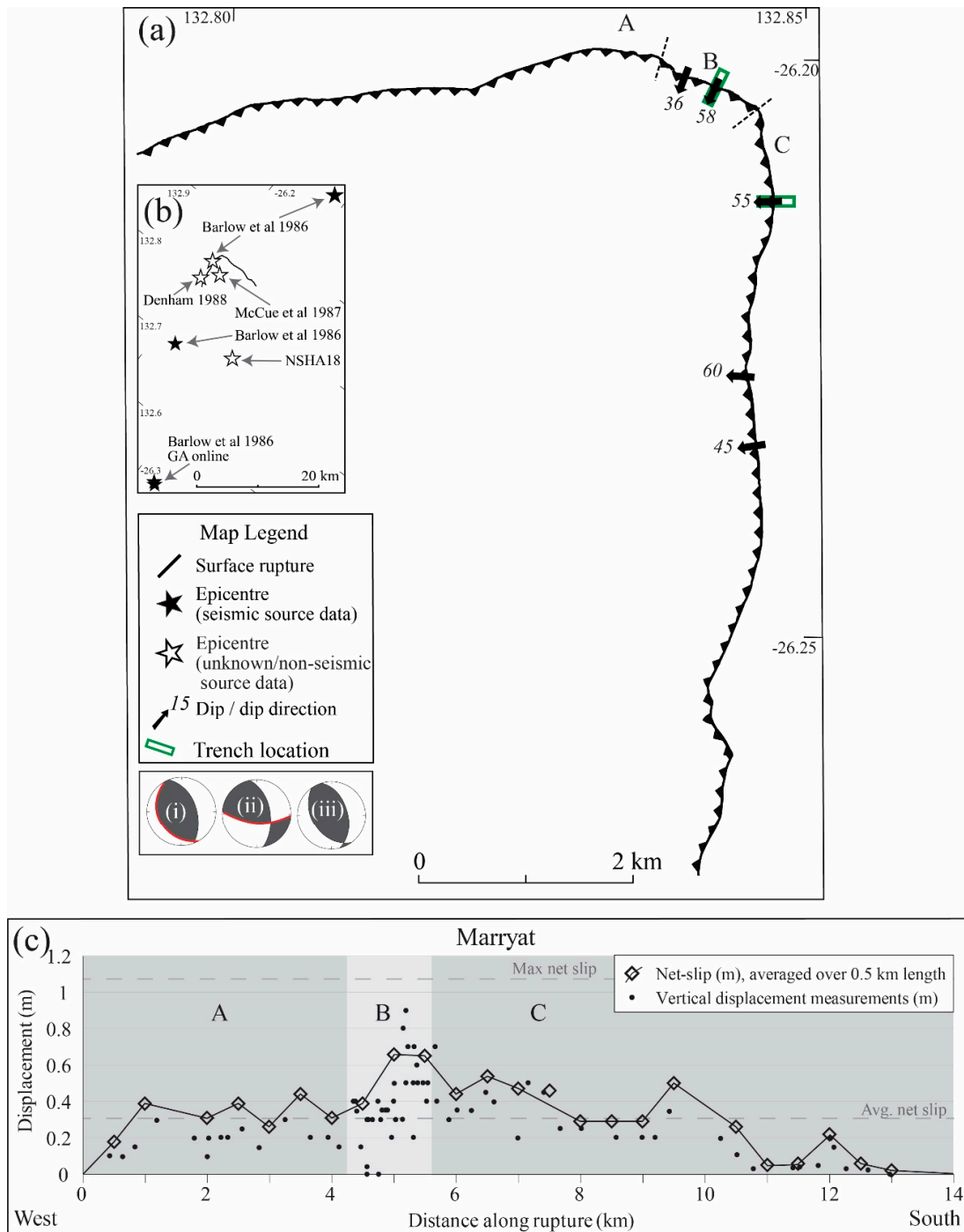


Figure 6. 1986 Mw 5.7 Marryat Creek earthquake (a) rupture and fracture map of Marryat Creek scarp and available dip measurements [48,118] with faults labelled as per displacement graphs, focal mechanisms (red line shows preferred plane from original publication) from (i) Fredrich et al., 1968, (ii) Barlow et al., 1986, (iii) CMT, trench location from [118], (b) published epicenter locations, and (c) graph of along-rupture vertical and lateral displacement measurements [48] and net slip calculated from available data averaged over 0.5 km increments (this study).

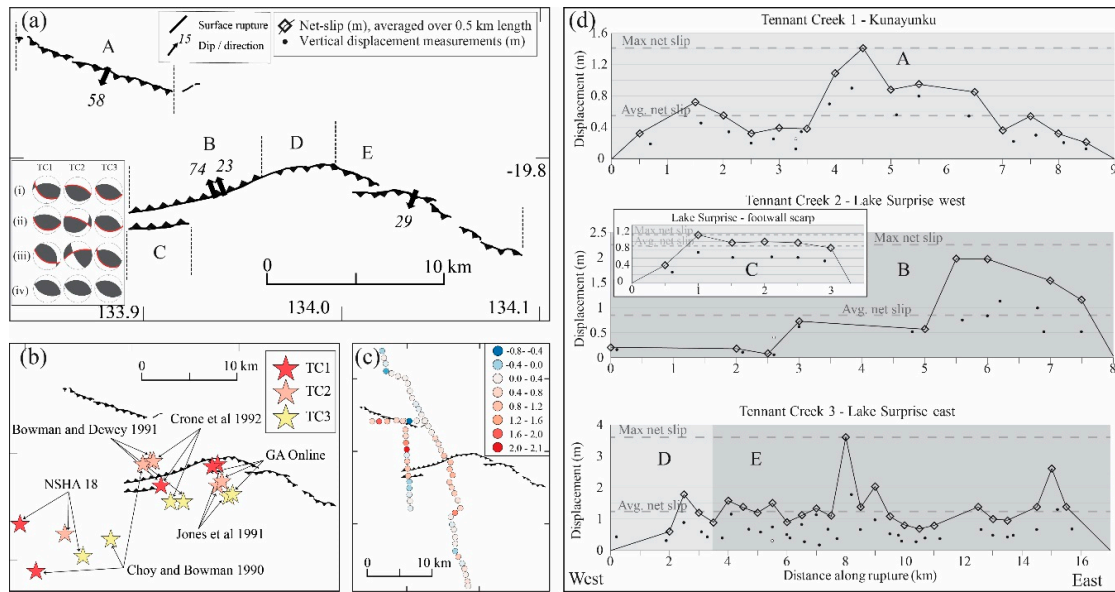


Figure 7. 1988 Mw 6.3 (TC1), 6.4 (TC2) and 6.6 (TC3) Tennant Creek earthquakes (a) rupture and cracking map of Kunayungku and Lake Surprise scarps with available dip measurements also the locations of trenches from [63] with faults labelled as per displacement graphs, focal mechanisms (red line shows preferred plane from original publication) from (i) McCaffrey 1989, (ii) Choy and Bowman 1990, (iii) Jones et al., 1991, (iv) CMT, (b) published epicenter locations of all three mainshocks (c) resurveyed benchmark offsets [63] uncertainties as discussed in text, and (d) graphs of along-rupture vertical and lateral displacement measurements [63] and net slip calculated from available data averaged over 0.5 km increments (this study).

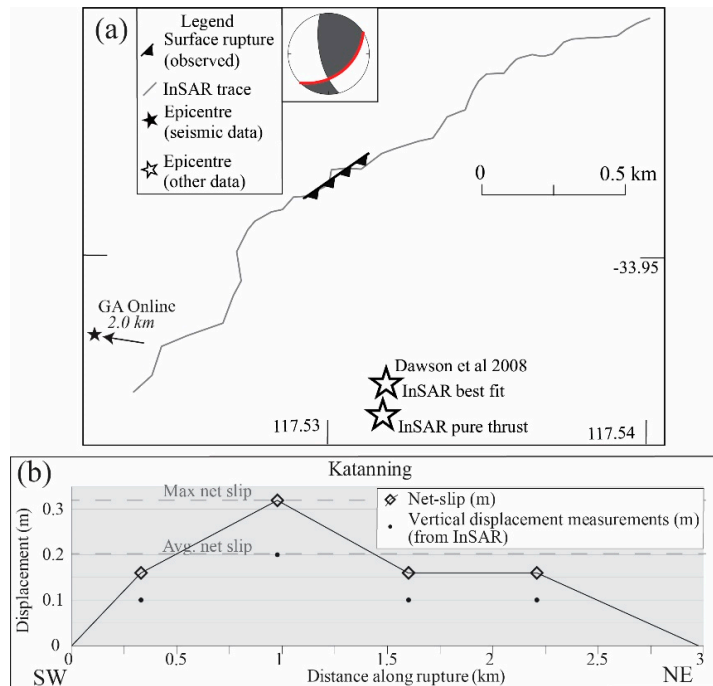


Figure 8. 2008 Mw 4.7 Katanning earthquake (a) approximate visible rupture and InSAR trace (digitized from [70]), published epicenter locations and focal mechanism [70] (b) graph of along-rupture vertical and displacement taken from InSAR data [70] and net slip calculated from InSAR data (this study).

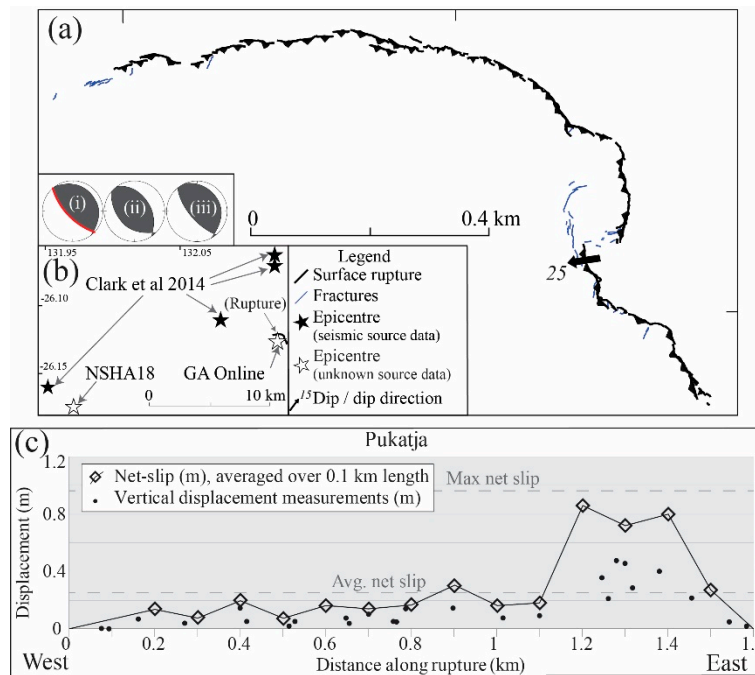


Figure 9. 2012 Mw 5.2 Pukatja/Ernabella earthquake (a) rupture and fracture map of Pukatja scarp and available dip measurements also the location of hand-dug trench [9], focal mechanisms as described in [9] from (i) Clark et al., 2014, (ii) GCMT, (iii) St Louis University; (b) graph of along-rupture vertical displacement measurements [9] and net slip calculated from available data averaged over 0.1 km increments (this study).

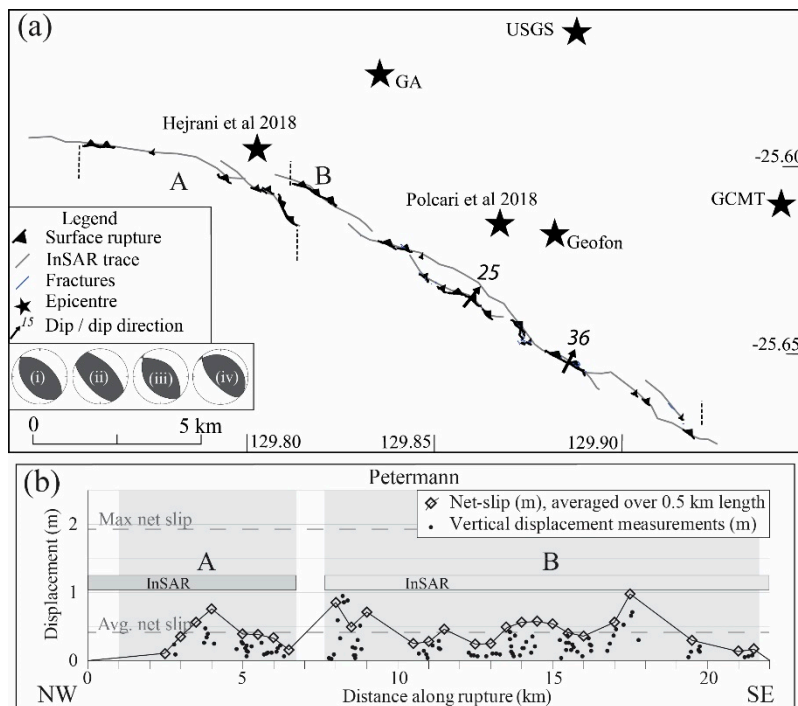


Figure 10. 2016 Mw 6.1 Petermann earthquake (a) rupture and fracture map of Petermann scarp [73] showing published epicenter locations and dip measurements of rupture (also the location of hand-dug trenches), focal mechanisms (i–iii) as described in [73], (i) USGS, (ii) GCMT, (iii) Geofon, and (iv) from Hejrani and Tkalčić 2018; (b) graph of along-rupture vertical displacement measurements and net slip calculated from available data averaged over 0.5 km increments.

Vertical and lateral offsets for all ruptures were digitized from primary literature (see EarthArXiv reports [120–126] for methods and uncertainties). New net-slip values were calculated for all ruptures from measured offsets, with dips assigned to each field offset measurement based on measured surface dips and/or focal mechanisms (dip measurements from primary literature shown on Figures 3–10 and in Table 6—preferred dip from this paper in Tables 1 and 6). Offset and net-slip data are presented in Figures 3–10 along with length weighted averages to reduce bias towards sections of scarp where high number of measurements were taken (generally where offset is higher). Average offset is between 42%–77% lower than the maximum offset for each rupture (Table 6). Displacement data are visually assigned a displacement profile shape [7] with six of ten ruptures best described by triangle profiles (2= symmetrical, 4= asymmetrical), two assigned an asymmetrical sine profile, and three best represented by a straight average profile (Table 6).

Offset data from resurveyed benchmarks (Tennant Creek [62]) and releveling along infrastructure (Meckering [25]) were digitized from original publications to visualize distributed deformation across the rupture zone (Figures 1 and 7). No uncertainties are reported for the Meckering data [25], though they are likely in the order of Tennant Creek where original authors report uncertainties of ± 9.3 –25 cm [62,136]. Despite large uncertainties, the authors of both datasets believe offsets constrain fault geometries and show distributed hanging-wall uplifts (and to a lesser extent, foot-wall depression).

3.4. Environmental Damage

Environmental damage as described in primary literature or visible in published photos for each event were classified under the ESI-07 Scale [10] and summarized in Table 7 (comprehensive details in EarthArXiv reports [120–126]). Seven of eleven historic ruptures (excluding Katanning) can be described as an ESI IX – X despite having a wide range of lengths, magnitudes, and displacements.

Fracturing/cracking is reported for all historic surface ruptures, but generally only in the immediate vicinity of the surface rupture, captured by the rupture ESI value. This may relate to a lack of far-field mapping but is considered to be fairly representative of the true spatial distribution based on described mapping campaigns. The Meckering and Petermann events have the most aerially extensive fracturing, with areas of 580 and 210 km² respectively. Of the total area covered by Meckering and Petermann fracturing, approximately 70% and 77% respectively is on the hanging-wall.

Where events occurred close to population centers (Meckering, Cadoux, Calingiri) ground water bores showed evidence of seismic fluctuation (no anomalies were identified in Tennant Creek bore data). The only observed liquefaction for any historic rupture comes from Meckering, where multiple sand blows were observed on the hanging-wall along the Mortlock River. Rockfalls are reported for three ruptures. Concentric or polygonal cracking was reported in the Meckering, Calingiri, Cadoux and Petermann events [25,41,73], and holes (possibly related to collapsible soils e.g., [137]) were reported along the rupture on the hanging-wall for Calingiri and Petermann [41,73]. It is possible that tree damage, hydrological effects, rock falls, polygonal cracking, or holes occurred for other ruptures than those listed but were not observed or described. Until the 2012 Pukatja event, field investigations immediately following the event were conducted by hard-rock geologists or seismologists not necessarily familiar with earthquake mapping techniques.

3.5. Paleoseismology and Slip Rate

In total, 14 trenches are described across the Meckering, Calingiri, Cadoux, Marryat Creek, Tennant Creek, Pukatja and Petermann ruptures (Table 8). Tennant Creek, Marryat Creek and Meckering are the only ruptures where detailed palaeoseismic work is published, including multiple trenches, luminescence dating, and soil descriptions and chemistry [37,63].

Table 7. Summary of environmental effects described for each rupture, assigned ESI level, and approximate area around, or distance from, rupture.

Name	Rupture		Fractures		Displaced Rocks		Sand Blows		Tree Shaking		Slope/Rock fall		Hydrology ¹		Holes [41,73]	Concentric Fracturing [25,41,73]	Vegetation Death/Root Tear along Rupture [9,25,47,48,63,73]
	ESI	Area (km ²)	ESI	Area (km ²)	ESI	Area (km ²)	ESI	Area (km ²)	ESI	Area (km ²)	ESI	Dist. (km)	ESI	Dist. (km)			
Meckering	X	190	VIII	580	–	–	V	100	●	–	IV	200	IV	200	–	□	□
Calingiri	IX	2	VII	3	*	–	–	–	–	–	–	–	–	–	□	□	□
Cadoux	IX	50	VI	55	–	–	–	–	●	–	–	–	IV	250	–	□	–
Marryat Creek	X	20	VII	20	–	–	–	–	–	–	–	–	–	–	–	–	□
Tennant Creek ^	X	160	VIII	160	–	–	–	–	–	–	–	–	●	–	–	–	□
Katanning,	VIII	0.2	–	–	–	–	–	–	–	–	–	–	–	–	–	–	–
Pukatja	IX	1	VII	1	–	–	–	–	*	–	VII	15	–	–	–	–	□
Petermann	X	12.5	VII	210	IX	290	●	–	VI	20	VII	20	–	–	□	□	□
Lake Muir	IX	–	*	–	–	–	–	–	*	–	–	–	*	–	–	–	–

^ Treating the three Tennant Creek scarps as individual or combined results in the same ESI values. Area given is for a combined scarp. Magnitude is for largest mainshock. ¹ Anomalous ground-water levels recorded following earthquake. – No data or observations published. □ Observations of damage outside of ESI-07 descriptions. ● Damage noted as explicitly not present. * Evidence of damage but no detailed description.

Table 8. Summary of available paleoseismic trenching.

Rupture	Ref.	Location	Bedrock			Sediments		Pre-Existing:		Possible Rup. Since 100 ka
			Desc.	Age	Depth (m) (HW/EW)	Desc.	Age *	Cenozoic Offset	Bedrock Offset	
Meckering 1	[34,36,37]	Tributary of river	Not exposed		>3	Fluvial sands	<u>Late Pleistocene</u>	No	No	N
Meckering 2	[34,36,37]	Farmland	Altered granite	Archean	<1.5	Ferricrete / sand	T?/Holocene	No	Maybe ¹	N
Calingiri	[25]							No	Maybe ¹	
Cadoux/Carter scarp	[41]	Farmland	Altered granite	Archean	<0.5	Sand/soil	Q?	No	No	
Cadoux/Tank scarp	[41]	Farmland	Granite	Archean	0?			No	No	
Marryat Creek west	[118]	10m N of dry creek	Altered gneiss	Proterozoic	<0.3	Ferricrete / eolian sand	T?/<130 ka	No	No	N
Marryat Creek south	[118]	'Near' dry creek	Altered greenstone	Proterozoic	<1.25	Ferricrete/gravel, eolian sand	T?/<130 ka	No	No	N
Kunayungku	[63]	Max vert. disp.	Altered sedimentary rock	Cambrian?	<2	Ferricrete/eolian sand	T?/<30 ka	No	No	N
Lake Surprise east	[63]	Max vert. disp.	Not exposed		>2	Ferricrete/eolian sand	T?/<46 ka	No	No	N
Lake Surprise west 1	[63]	Monoclinal rupture (near quartz ridge)	Altered "iron-rich quartzite"	Cambrian?	<0.5/>2	Gravel/eolian sand	Q/<50 ka	No	Yes ³	Y
Lake Surprise west 2	[63]	Discrete rupture (375m E LSW-1)	Altered "hematitic quartzite"	Cambrian?	<0.5/>0.7	Ferricrete/gravel/eolian sand	T?/Q/<50 ka	Maybe ²	Yes ³	Y
Pukatja	[9]	Max. vert. disp.	Not exposed		>1.5	Sand	<u>~10⁴–10⁵</u>	No	No	Y
Petermann 1	Unpub.	Paleovalley	Not exposed		>1.5	Calcrete/eolian sand	T?/Q	No	No	N
Petermann 2	Unpub.	Inter-dune region	Not exposed		>1.5	Calcrete/eolian sand	T?/Q	No	No	N

* ages in bold from direct dating in literature, italics inferred based on nearby dating, underline from estimate in literature, "T?" or "Q?" estimated Tertiary or Quaternary. ¹ Thicker soil horizons described on foot-wall relative to hanging-wall [25]. ² Fissure of potentially seismic origin filled with gravel, overlain by eolian sand; fracture through ferricrete overlain by gravel and eolian sand [63]. ³ Authors propose three possible origins: earthquake rupture bedrock offset; paleochannel along pre-existing bedrock structure; or combination of both; paleotopography greater than twice the height of historic slip [63].

Of seven ruptures with detailed trench data (Table 8), five show evidence of no rupture since the lake Pleistocene (Meckering, Marryat Creek, Kunayungku, Lake Surprise east, Petermann). The only evidence of a pre-existing bedrock scarp exposed in any trench occurs in the second Lake Surprise west trench, and no clear evidence was found to support a seismic-offset origin for this topography (see EarthArXiv report [126] for more detail). Penultimate ruptures since 100 ka are possible for two of seven of these earthquake events, where sediments are estimated to be <100 ka in age, and where either no ferricrete/bedrock is exposed (Pukatja), or a bedrock scarp exists prior to overlying sedimentation (Lake Surprise west) (Table 8).

Maximum slip rates are calculated by applying minimum and maximum erosion rates for bedrock to determine the amount of slip (from average observed historic slip (Table 6)) that could have accumulated and been removed in the past million years. Minimum (0.3 m Myr^{-1}) and maximum (5.7 m Myr^{-1}) cosmogenic nuclide erosion rates from crystalline bedrock inselbergs across the Precambrian crust of central Australia (Figure 1) [138] are applied for ruptures where crystalline basement is exposed in trenches or observed at the surface within two meters of rupture (implying shallow bedrock). Where trenching exposed ferricrete or quartzite, cosmogenic nuclide erosion rates for quartzite exposed on flat bedrock summits in the Flinders Ranges are applied ($5\text{--}10 \text{ m Myr}^{-1}$) [109].

Applying erosion rates from inselbergs and quartzite bedrock summits to surface bedrock across the different cratonic and erosional environments in which ruptures occurred (e.g., Figure 1) introduces uncertainties that are unavoidable due to a lack of more appropriate erosion data. Based on a lack of evidence of any preceding ruptures for any of the historic events, including topographic or geomorphic, we prefer the minimum erosional estimates, giving maximum slip rates of $0.2\text{--}9.1 \text{ m Myr}^{-1}$.

Table 9. Maximum slip rates based on minimum and maximum bedrock erosion rates [109,138] and length-weighted average net-slip values (Table 6).

Name	Rate Applied *	Mw	Pref. Length (km)	Avg. Net-Slip (m)	Maximum Slip Rate (m/Myr)		
					Min.	Max.	Mean
Meckering	CB	6.59	40 ± 5	1.78	0.2	3.2	1.7
Calingiri	CB	5.03	3.3 ± 0.2	0.46	0.7	12.4	6.6
Cadoux	CB	6.1	20 ± 5	0.45	0.7	12.7	6.7
Marryat Creek	CB	5.7	13 ± 1	0.31	1	18.4	9.7
Kunayungku	Q	6.27	9 ± 1	0.55	9.1	18.2	13.7
Lake Surprise west	Q	6.44	9 ± 2	0.84	6	11.9	8.9
Lake Surprise east *	Q	6.58	16 ± 0.5	1.23	4.1	8.1	6.1
Katanning (InSAR)	CB	4.7	0.5 ± 0.5	0.2	1.5	28.5	15
Pukatja	CB	5.18	1.3 ± 0.3	0.25	1.2	22.8	12
Petermann	CB	6.1	21 ± 0.5	0.42	0.7	13.6	7.2

* Erosion rate for crystalline basement (CB) [138]; erosion rate for quartzite (Q) [109].

4. Discussion-Lessons from the Last 50 Years of Australian Surface Ruptures

4.1. Inconsistencies in Data Use

A number of inconsistent uses of data were found while reviewing papers that reference primary sources, as summarized below:

- Some of the original Marryat Creek vertical offset measurements are reproduced incorrectly in subsequent publications [7,118]. We recommend referring to the original source [48] or the data tables from this paper.
- Limbs of the Marryat Creek rupture show sinistral (west limb) and dextral (south limb) components due to SW over NE directed uplift along an arcuate rupture (best described as three faults, Figures 2

and 6). Data tables used in subsequent scaling relationships [6] describe the event as left-lateral based on one of three published focal mechanisms. We recommend a dominantly reverse mechanism for this event based on all available data.

- We recommend referring to the original source of the Calingiri focal mechanism [23] when describing kinematics and preferred rupture plane geometry, as subsequent authors [25] appear to misread the mechanism [121].
- The Tennant Creek rupture has been treated by multiple authors as a single rupture length for fault scaling relationships [7,8,104,139,140] and hazard mapping [119,141,142] as opposed to three separate earthquakes and associated ruptures [6,143–145], a decision which significantly changes the length to magnitude ratio and slip distribution relative to an averaged epicentre location and magnitude.
- An instance of the above decision is seen where a 6 km step over between Tennant Creek scarps is identified as an outlier for reverse fault data [7]. The rupture length and complexity for this event is not anomalous if treated as three separate events.
- Some scaling relationships (e.g., [7]) define only a portion of the Cadoux scarp (the 10km long Robb Scarp), due to “insufficient mapping” of the northern ~6 km. The full rupture includes one step-over that fits the publication analysis criteria (>1 km) but is not represented in the original paper’s database [7] and subsequent work [8,139,146]. Mapping of the Cadoux rupture was thorough, but uncertainty regarding which of the mapped scarps (if any) represent the Cadoux mainshock fault complicates the use of this event in scaling relationships.
- A slip rate of 0.005 mm/yr is used to describe the Marryat Creek scarp [147]. This value is likely derived from ~0.5 m measured historic slip in a trench with no evidence of prior rupture between deposition of Quaternary sediments (estimated age from primary source < 130 ka [63]) and formation of the structure along which the modern event ruptured (Proterozoic) [118]. While evidence of prior Quaternary–Tertiary rupture may have been removed by erosion, a slip rate of 0.5 m per 100,000 years is unsupported by available evidence.
- The recently published NSHA18 applies slip rates of 4–8 m/Myr for the historic ruptures discussed in this paper [119,141]. No historic surface ruptures provide convincing evidence of rupture between deposition of Quaternary sediments (50 ka to late Pleistocene) and formation of the host structure (Archean–Cambrian). At least for cratonic areas of Australia (Figure 1), questions arise as to whether historically seismogenic faults are recurrent at all, or if long-term seismic release may be hosted across unique basement structures (e.g., [4]), as well as on recurrent structures (e.g., Lort River, Hyden, Dumbleyung [2,34,108]). We recommend caution in applying these rates in future work.

4.2. Surface rupture Bedrock Controls, Updated Datasets and Environmental Intensity

Analysis of geology and reanalysis of mapped ruptures presented in this paper suggest that in four of the ten events studied (Meckering, Marryat Creek, Cadoux and Peterman) rupture propagated across 2–6 bedrock-controlled faults (e.g., pre-existing fractures and/or foliation planes and/or lithological boundaries and/or intrusive boundaries), and nine of ten events show strong basement controls on rupture location and orientation. Simplistic projection of surface defined faults using our preferred dips results in faults intersecting at depths that are consistent with published centroid depths (e.g., <4 km) in three of the four events with more than one fault defined (Petermann excluded). In all four cases, fault intersections project up-dip to the area of maximum vertical offset (in the case of Petermann, maximum dip occurs where the two faults overlap). It is uncertain with available seismic data whether hypocenters align with these projected fault intersections, and more data would be required to show that surface defined faults can be extended to depth along planar slip zones. However, linear geophysical anomalies in many cases show ruptures associated with basement conjugate fracture/dike orientations underlying rupture, suggesting strong control of the crustal architecture on intraplate earthquake nucleation and/or propagation.

New length, dip, and net-slip data presented for historic ruptures are derived by applying consistent framework and methodology. Past scaling relationships have included and excluded

Australian surface rupturing events inconsistently, generally without clear explanation. They have also relied on vertical offset measurements as most of the original publications do not calculate net-slip. Length-weighted averages of net-slip values calculated in this paper are 32%–67% larger than those for vertical offset data, and maximum net-slip is 68%–89% higher than maximum vertical offset. This suggests that Australian events may be systematically misrepresented in past scaling relationships. Our new data, compiled by thorough analysis of available seismological and field data, and coupled with the recent revision of magnitude values [11], will facilitate more consistent integration of Australian events into earthquake catalogues and displacement-length scaling relationships.

In Table 10 we compare the calculated M_w , area and average displacement from SCR dip-slip scaling relationships of [148] using the surface rupture length used in developing the scaling relationships with the length from this paper. Table 10 then compares the difference between calculated average displacement and magnitude as derived using length of this paper and SCR dip-slip scaling relationship [148] with the average net slip derived from this paper, and update M_w values [11]. Results show differences of over 600% between scaling relationship average displacement and calculated average net slip values of this paper, and up to 18.7% difference in calculated M_w and updated values [11]. This highlights the need to investigate length, magnitude, and net-slip inputs of previous scaling relationships.

Most vertical displacement data for historic surface ruptures are collected as spot-height measurements of foot-wall elevation relative to hanging-wall elevation proximal to the surface trace. Less frequently, scarp perpendicular profiles are captured 5–50 m either side of the rupture. Satellite-based imaging of recent scarps (Petermann [75,77,78], Katanning [70], Lake Muir ([79])) shows permanent distributed displacement of the hanging-wall, and to a lesser degree of the foot-wall that is not captured by these spot-heights and short traverses. Specifically, InSAR imaging shows distributed deformation extending hundreds of metres to kilometres perpendicular to surface scarps [78], and extending along-strike for kilometres beyond the surface rupture detectable in the field [70,78,79]. This is particularly the case for smaller earthquakes (Katanning [70] (Figure 8) and Lake Muir (in review [79])), where the rupture ellipse only partially intersects the surface. Without these satellite derived deformation imaging techniques, the degree to which field observations and spot-height measurements along the visible surface rupture underestimate the length, height and width of surface deformation along a fault cannot be quantified.

Digitized offset data from resurveyed benchmarks across the Tennant Creek (Figure 7), Meckering (Figure 3) and Cadoux (EarthArXiv report [122]) ruptures provide evidence of distributed hanging-wall offset, though published uncertainties are on the order of measured offsets and data should be interpreted with caution. This data cannot be improved upon within the resolution of pre-deformation height data but suggests that the deformation envelope extends beyond the discrete surface rupture, and offset measurements as presented in Figures 3–10 may underestimate the true total vertical displacement values for each event. The ratio of distributed deformation to discrete deformation at a rupture tip might be expected to be larger for surface rupture segments that are more modest in vertical displacement, or cut through relatively more weathered regolith or thicker sedimentary deposits, as much of the initial deformation will be taken up as folding prior to the emergence of the fault tip [149].

This paper reviews primary literature to identify environmental earthquake effects (EEEs) for the purposes of applying the ESI-07 Scale [10,150] to Australian surface rupturing earthquakes. We find that the majority of environmental damage is observed in the immediate rupture zone, with the exception of rare rockfalls in prone-areas (e.g., road cuttings) at distances of ~200 km, and rare ground-water fluctuations up to 250 km away for some but not all events where ground water data was investigated. While this dataset likely does not capture the full range of potential ESI values and affected area due to sparse reporting of EEEs in the literature, it does provide a basis for comparing the maximum ESI and magnitude of reverse earthquakes in intraplate, low-topography, near-surface crystalline bedrock (in most cases), and generally arid settings against events in tectonically and geomorphically diverse regions (e.g., [151–159]).

Table 10. Comparisons between calculated magnitude, area and displacement from previous length scaling relationship [148] using surface rupture length from [148] and length from this paper.

Name	Leonard 2014 [148]		Calculated [148]			This Paper	Calculated (This Paper)			Percent Difference Calculated			Avg. Net Slip ⁵	% Diff ⁶	M _w [11]	% Diff ⁶
	SRL ¹ (km)	Source	M _w ²	A ³ (km ²)	D ⁴ (m)	L (km)	M _w ²	A ³ (km ²)	D ⁴ (m)	M _w	A (km ²)	D (m)				
Meckering	37	[160]	6.93	5546	5.44	40	6.99	6316	5.8	0.9%	12.2%	6.3%	1.78	-225.8%	6.59	-6.1%
Calingiri	3.3	[160]	5.18	99	0.73	3.3	5.18	99	0.73	0.0%	0.0%	0.5%	0.46	-58.7%	5.03	-3.0%
Cadoux	14	[160]	6.23	1098	2.42	20	6.49	1989	3.26	4.0%	44.8%	25.8%	0.45	-624.4%	6.1	-6.4%
Marryat Creek	13	[160]	6.18	970	2.27	13	6.18	970	2.27	0.0%	0.0%	-0.2%	0.31	-632.3%	5.7	-8.4%
Kunayungku	10.2	[160]	6	648	1.86	9	5.91	526	1.67	-1.5%	-23.2%	-11.3%	0.55	-203.6%	6.27	5.7%
Lake Surprise west	6.7	[160]	5.7	321	1.31	9	5.91	526	1.67	3.6%	39.0%	21.7%	0.84	-98.8%	6.44	8.2%
Lake Surprise east *	16	[160]	6.33	1372	2.70	16	6.33	1372	2.7	0.0%	0.0%	-0.1%	1.23	-119.5%	6.58	3.8%
Katanning (InSAR)	1.26	[70]	4.49	20	0.33	0.5	3.82	4	0.15	-17.5%	-400.0%	-117.6%	0.2	25.0%	4.7	18.7%
Pukatja	1.6	[9]	4.66	30	0.40	1.3	4.51	21	0.33	-3.3%	-42.9%	-21.2%	0.25	-32.0%	5.18	12.9%

¹ Surface rupture length. ² [148]: $M_w = a + b \cdot \log(L)$. ³ [148]: $A = C_1 L^{1+\beta}$. ⁴ [148]: $D = C_2 A^{1/2}$. ⁵ Average net slip calculated in this paper (Table 6). ⁶ Percent difference between calculated average displacement and M_w using length of this paper [148], and average net slip calculated in Table 6, and M_w of [11].

4.3. Recurrence of Historic Surface Ruptures and Implications for Hazard Modelling

In the fifty years between 1968 and 2018, eleven moderate magnitude reverse earthquakes caused surface ruptures in cratonic Australian. Nine of the ten events analyzed show evidence of rupture along pre-existing structures with little to no evidence of prior Neotectonic movement. While this does not preclude the possibility that evidence of prior rupture was removed prior to the late Pleistocene, the lack of topographic or geomorphic evidence supporting repeated rupture suggests historic surface ruptures may have occurred on faults that could be considered previously inactive in the Neotectonic period (e.g., [4]).

It is unclear whether the historic surface rupturing faults have entered a period of activity and will host future Neotectonic earthquakes, have occurred as isolated events, or have such long recurrence intervals as to obscure all evidence of prior rupture. Paleoseismic work across the Precambrian SCR crust (Figure 1) has shown that faults in similar settings as the historic ruptures have hosted multiple Neotectonic earthquakes [2,34,108], with available dating indicating long recurrence (>30–70 ka [2]), and low topography indicating erosion may outpace seismic slip-rate. In contrast, paleoseismic investigations in the Phanerozoic non-extended crust of eastern Australia identify multiple faults with recurrence frequent enough to maintain topography [3,5,34,101,107,109], despite no historic surface rupturing or large earthquakes in this part of the continent.

Historic surface rupture kinematics are all consistent with S_{Hmax} (as measured from bore-hole breakouts, drilling induce fractures, and focal mechanisms [100]) either directly (e.g., a straight fault perpendicular to S_{Hmax}) or indirectly (e.g., rupture occurred along multiple faults, some of which are aligned oblique to S_{Hmax} , but uplift of the hanging-wall block is perpendicular to S_{Hmax}). The past fifty years of historic surface rupturing events show that in the Precambrian non-extended crust, basement with at least one set of linear structures aligned with S_{Hmax} , or multiple conjugate basement structures, could host a shallow moderate magnitude surface rupturing earthquake along one or multiple (in these cases, previously unrecognized and typically unrecognizable) faults. Eight of eleven surface rupturing earthquakes have occurred in areas of (or proximal to) preceding seismicity, while three (Petermann, Pukatja and Marryat Creek) occurred in areas with low historic seismicity, though instrument density limits the magnitude of completeness and location accuracy and precision of the historic earthquake catalogue in these locations. This suggests that spatially smoothed (distributed) seismicity models may provide the best utility for seismic hazard analyses in the central and western parts of Australia (e.g., [161]). This is also relevant for assessments of earthquake hazard in Precambrian intraplate crust elsewhere (e.g., Canada [162–164]). Further work is required to understand tentative correlations between seismogenic potential and large geophysical anomalies and/or Moho discontinuities (e.g., [165,166]), and whether transient local stress perturbations increase the potential for shallow seismicity (e.g., changes in pore-fluid pressure [76] or surface load variations [4]).

The historic earthquake catalogue for Australia is complete for $M_L > 5.5$ since 1910, and $M_L > 5.0$ since 1960 [102]. The magnitude values of historic earthquakes were recently revised [11]. This new catalogue contains seven $M_W > 5.5$ on-shore earthquakes within the Precambrian non-extended crust that are not related to the historic surface rupturing events, and only one onshore event in the eastern Phanerozoic crust (Figure 1). The Precambrian crustal events include: four events (1941 M_W 5.6, 5.9, 6.5, and 1972 M_W 5.6) in the Simpson Desert NT [80,83,167], one event (1970 M_W 5.9) within the Lake Mackay WA sequence (20 events M_W 4.5–5.5 between 1970–1992) [23,81,83,167], one event 200 km south of Warburton WA (1975 M_W 5.6), and the 1941 M_W 6.8 Meeberrie WA event—Australia's largest recorded onshore earthquake (Figure 1). No surface ruptures have been identified for these events. While depths are poorly constrained due to poor instrumental density, estimates range from 7–33 km [11,83], deeper than the best estimates of depth for surface rupturing events (1–4 km for centroids, <6 km for hypocentral/base of fault depth). This suggests that moderate magnitude and potentially damaging earthquakes (e.g., $M_W > 5.5$) can be generated at depths of up to 33 km within the Precambrian non-extended crust, providing another source of hazard that cannot be effectively captured by active-fault catalogues in seismic hazard analysis.

5. Conclusions

We provide new length, dip, and net-slip data derived using a consistent framework and methodology in order to facilitate more consistent integration of Australian events into earthquake catalogues and displacement-length scaling relationships. Our reanalysis of primary data from 67 publications on ten of eleven historical surface rupturing earthquakes in Australia shows:

- Surface rupture fault orientations aligned with basement structures identified in proximal surface outcrops (foliations \pm quartz veins \pm intrusive boundaries \pm pre-existing faults) and linear geophysical anomalies;
- Rupture involve 1–6 discrete faults based on reanalysis of surface rupture lengths using consistent criteria, with evidence that intersecting basement structures may control rupture initiation and/or propagation;
- Large aleatoric and epistemic uncertainties in seismological data, related to a sparse seismic network, limit determination of hypocenter and fault interaction, rupture propagation, and assessment of whether surface ruptures project to seismogenic depths along planar principle slip zones or whether rupture propagates to multiple basement structures in the near-surface;
- Available analyses of rupture centroids (seven of ten events) show depths of 1–4 km indicating predominately shallow seismic moment release;
- None of the historic surfacing rupturing events have unambiguous geological or geomorphic evidence for preceding earthquakes on the same faults, with five events showing an absence of rupture since at least the late Pleistocene;
- Within the constraints of available basement erosion rates, preferred maximum slip rates are 0.2–9.1 m Myr⁻¹ with an estimated minimum epistemic uncertainty of at least one order of magnitude lower. These are considered applicable only within the non-extended Precambrian crust in which all historic surface ruptures have occurred;
- ESI-07 estimates range by ± 3 classes in each earthquake and provide new maximum ESI vs. magnitude data for comparison between different tectonic and geomorphic settings;

Supplementary Materials: The following are available online at <http://www.mdpi.com/2076-3263/9/10/408/s1>.

Author Contributions: Conceptualization, M.Q. and T.R.K.; methodology, T.R.K.; validation T.R.K. and D.C.; formal analysis, T.R.K.; investigation, T.R.K.; data curation T.R.K.; writing—original draft preparation, T.R.K.; writing—review and editing, T.R.K., M.Q. and D.C.; visualization, T.R.K. and M.Q.; supervision, M.Q.; project administration, T.R.K. and M.Q.; funding acquisition, M.Q.

Funding: This research was funded by the Australian Research Council through Discovery Grant #DP170103350. T. King received funding through the Australian Government Research Training Program Scholarship.

Acknowledgments: The authors thank the editors and three reviewers for comments that improved this work. We would like to acknowledge the Noongar people of south-west Western Australia, the Warumungu people of Tennant Creek, and the Antakirinja, Yankunytjatjara, and Pitjantjatjara people of the Western Desert and APY lands in South Australia/Northern Territory, as the traditional custodians of the land on which all historic surface ruptures occurred, and where the data described in this paper were collected. D. Clark publishes with the permission of the Chief Executive Officer of Geoscience Australia.

Conflicts of Interest: The authors declare no conflict of interest.

References

1. Crone, A.J.; Machette, M.N.; Bowman, J.R. Episodic nature of earthquake activity in stable continental regions revealed by palaeoseismicity studies of Australian and North American quaternary faults. *Aust. J. Earth Sci.* **1997**, *44*, 203–214. [[CrossRef](#)]
2. Crone, A.J.; De Martini, P.M.; Machette, M.N.; Okumura, K.; Prescott, J.R. Paleoseismicity of Two Historically Quiescent Faults in Australia: Implications for Fault Behavior in Stable Continental Regions. *Bull. Seismol. Soc. Am.* **2003**, *93*, 1913–1934. [[CrossRef](#)]
3. Quigley, M.C.; Clark, D.; Sandiford, M. Tectonic geomorphology of Australia. *Geol. Soc. Lond. Spec. Publ.* **2010**, *346*, 243–265. [[CrossRef](#)]

4. Calais, E.; Camelbeeck, T.; Stein, S.; Liu, M.; Craig, T.J. A new paradigm for large earthquakes in stable continental plate interiors. *Geophys. Res. Lett.* **2016**, *43*, 10621–10637. [[CrossRef](#)]
5. Clark, D.; McPherson, A.; Van Dissen, R.J. Long-term behaviour of Australian stable continental region (SCR) faults. *Tectonophysics* **2012**, *566–567*, 1–30. [[CrossRef](#)]
6. Wells, D.L.; Coppersmith, K.J. New Empirical Relationships among Magnitude, Rupture Length, Rupture Width, Rupture Area, and Surface Displacement. *Bull. Seismol. Soc. Am.* **1994**, *84*, 974–1002.
7. Wesnousky, S.G. Displacement and geometrical characteristics of earthquake surface ruptures: Issues and implications for seismic-hazard analysis and the process of earthquake rupture. *Bull. Seismol. Soc. Am.* **2008**, *98*, 1609–1632. [[CrossRef](#)]
8. Biasi, G.P.; Wesnousky, S.G. Steps and gaps in ground ruptures: Empirical bounds on rupture propagation. *Bull. Seismol. Soc. Am.* **2016**, *106*, 1110–1124. [[CrossRef](#)]
9. Clark, D.; Mcpherson, A.; Allen, T.; De Kool, M. Coseismic surface deformation caused by the 23 March 2012 Mw 5.4 Ernabella (Pukatja) earthquake, central Australia: Implications for fault scaling relations in cratonic settings. *Bull. Seismol. Soc. Am.* **2014**, *104*, 24–39. [[CrossRef](#)]
10. Michetti, A.M.; Esposito, E.; Guerrieri, L.; Porfido, S.; Serva, L.; Tatevossian, R.E.; Vittori, E.; Audemard, F.A.; Azuma, T.; Clague, J.; et al. *Intensity Scale ESI 2007*; Guerrieri, L., Vittori, E., Eds.; APAT: Rome, Italy, 2007; Volume 74.
11. Allen, T.; Leonard, M.; Ghasemi, H.; Gibson, G. *The 2018 National Seismic Hazard Assessment: Earthquake Epicentre Catalogue (GA Record 2018/30)*; Geoscience Australia, Commonwealth of Australia: Canberra, Australia, 2018. [[CrossRef](#)]
12. Everingham, I.B. *Preliminary Report on the 14 October 1968 Earthquake at Meckering, Western Australia (BMR Record 1968/142)*; 1968/142; Bureau of Mineral Resources, Geology and Geophysics Canberra: Canberra, Australia, 1968. Available online: <http://pid.geoscience.gov.au/dataset/ga/12254> (accessed on 2 August 2019).
13. Gordon, F.R. *Reconstruction of Meckering Town, a Geological Appraisal (GSWA Record 1968/14)*; Geological Survey of Western Australia: Perth, Western Australia, 1968.
14. Conacher, A.J.; Murray, I.D. The Meckering earthquake, Western Australia, 14 October 1968. *Aust. Geogr.* **1969**, *11*, 179–184. [[CrossRef](#)]
15. Everingham, I.B.; Gregson, P.J.; Doyle, H.A. Thrust Fault Scarp in the Western Australian Shield. *Nature* **1969**, *223*, 701–703. [[CrossRef](#)]
16. Lewis, J.D. *The Geology of the Country around Meckering (GSWA Record 1969/18)*; Geological Survey of Western Australia: Perth, Western Australia, 1969.
17. Gordon, F.R. Water level changes preceding the Meckering, Western Australia, earthquake of October 14, 1968. *Bull. Seismol. Soc. Am.* **1970**, *60*, 1739–1740.
18. Everingham, I.B.; Gregson, P.J. *Meckering Earthquake Intensities and Notes on Earthquake Risk for Western Australia (BMR Report 1970/97)*; Bureau of Mineral Resources, Geology and Geophysics: Canberra, ACT, Australia, 1970. Available online: <http://pid.geoscience.gov.au/dataset/ga/12510> (accessed on 2 August 2019).
19. Gordon, F.R. Faulting during the earthquake at Meckering, Western Australia: 14 October 1968. *Bull. R. Soc. N. Z.* **1971**, *9*, 85–93.
20. Gordon, F.R.; Wellman, H.W. A mechanism for the Meckering earthquake. *R. Soc. N. Z. Bull.* **1971**, *9*, 95–96.
21. Everingham, I.B.; Gregson, P.J. *Mundaring Geophysical Observatory, Annual Report, 1968 (BMR Record 1971/12)*; Bureau of Mineral Resources, Geology and Geophysics: Canberra, Australia, 1971. Available online: <http://pid.geoscience.gov.au/dataset/ga/12549> (accessed on 2 August 2019).
22. Gregson, P.J.; McCue, K.; Smith, R.S. *An Explanation of Water Level Changes Preceding the Meckering Earthquake of 14 October 1968 (BMR Record 1972/101)*; Bureau of Mineral Resources, Geology and Geophysics: Canberra, Australia, 1972. Available online: <http://pid.geoscience.gov.au/dataset/ga/12782> (accessed on 2 August 2019).
23. Fitch, T.J.; Worthington, M.H.; Everingham, I.B. Mechanisms of Australian earthquakes and contemporary stress in the Indian ocean plate. *Earth Planet Sci. Lett.* **1973**, *18*, 345–356. [[CrossRef](#)]
24. Denham, D.; Alexander, L.G.; Worotnicki, G. The stress field near the sites of the Meckering (1968) and Calingiri (1970) earthquakes, Western Australia. *Tectonophysics* **1980**, *67*, 283–317. [[CrossRef](#)]
25. Gordon, F.R.; Lewis, J.D. *The Meckering and Calingiri Earthquakes October 1968 and March 1970*; Geological Survey of Western Australia: Perth, Australia, 1980.
26. Vogfjord, K.S.; Langston, C.A. The Meckering earthquake of 14 October 1968: A possible downward propagating rupture. *Bull. Seismol. Soc. Am.* **1987**, *77*, 1558–1578.

27. Langston, C.A. Depth of Faulting during the 1968 Meckering, Australia, earthquake sequence determined from waveform analysis of local seismogram. *J. Geophys. Res.* **1987**, *92*, 11561–11574. [CrossRef]
28. Fredrich, J.; Mccaffrey, R.; Denham, D. Source parameters of seven large Australian earthquakes determined by body waveform inversion. *Geophys. J.* **1988**, *95*, 1–13. [CrossRef]
29. Gregson, P.J. (Ed.) *Recent intraplate seismicity studies symposium, Perth, Western Australia September 1990 (BMR Record 1990/44)*; Bureau of Mineral Resources, Geology and Geophysics: Canberra, ACT, Australia, 1990. Available online: <http://pid.geoscience.gov.au/dataset/ga/14335> (accessed on 2 August 2019).
30. Lewis, J.D. Meckering revisited. Recent Intraplate Seismicity Studies Symposium, Perth Western Australia (BMR Record 1990/44). 1990. Available online: <http://pid.geoscience.gov.au/dataset/ga/14335> (accessed on 2 August 2019).
31. Lewis, J.D. *The Meckering Earthquake of 17 January 1990 (GSWA Record 1990/6)*; Geological Survey of Western Australia: Perth, Western Australia, 1990.
32. Dent, V.F. Foreshocks and aftershocks of the 17 Jan 1990 Meckering earthquake. In *Recent Intraplate Seismicity Studies Symposium, Perth Western Australia (BMR Record 1990/44)*; Gregson, P.J., Ed.; Bureau of Mineral Resources, Geology and Geophysics: Canberra, ACT, Australia, 1990. Available online: <http://pid.geoscience.gov.au/dataset/ga/14335> (accessed on 2 August 2019).
33. Dentith, M.; Clark, D.; Featherstone, W.E. Aeromagnetic mapping of Precambrian geological structures that controlled the 1968 Meckering earthquake (Ms 6.8): Implications for intraplate seismicity in Western Australia. *Tectonophysics* **2009**, *475*, 544–553. [CrossRef]
34. Clark, D.; Mcpherson, A.; Collins, C. *Australia's Seismogenic Neotectonic Record: A Case for Heterogeneous Intraplate Deformation (GA Record 2011/11)*; Geoscience Australia, Commonwealth of Australia: Canberra, Australia, 2011. Available online: <http://pid.geoscience.gov.au/dataset/ga/70288> (accessed on 2 August 2019).
35. Johnston, J.F.; White, S.R. *Understanding the Meckering Earthquake: Western Australia, 14 October 1968*; Geological Survey of Western Australia: Perth, Australia, 2018. [CrossRef]
36. Clark, D. *What Have We Learned in the 50 Years since the 1968 Meckering Earthquake?* Geoscience Australia, Commonwealth of Australia: Canberra, Australia, 2018. Available online: <http://pid.geoscience.gov.au/dataset/ga/123342> (accessed on 2 August 2019).
37. Clark, D.; Edwards, M. *50th Anniversary of the 14th October 1968 Mw 6.5 (Ms 6.8) Meckering Earthquake (GA Record 2018/39)*; Geoscience Australia, Commonwealth of Australia: Canberra, ACT, Australia, 2018. Available online: <http://dx.doi.org/10.11636/Record.2018.039> (accessed on 2 August 2019).
38. Everingham, I.B.; Parkes, A. *Intensity Data for Earthquakes at Landor (17 June 1969) and Calingiri (10 March 1970) and Their Relationship to Previous Western Australian Observations (BMR Record 1971/80)*; 1971/80; Bureau of Mineral Resources, Geology and Geophysics: Canberra, Australia, 1971. Available online: <http://pid.geoscience.gov.au/dataset/ga/12617> (accessed on 2 August 2019).
39. Gregson, P.J. *Mundaring Geophysical Observatory Annual Report, 1970 (BMR Record 1971/77)*; Bureau of Mineral Resources, Geology and Geophysics: Canberra, Australia, 1971. Available online: <http://pid.geoscience.gov.au/dataset/ga/12614> (accessed on 2 August 2019).
40. Gregson, P.J.; Paull, E.P. *Preliminary Report on the Cadoux Earthquake, Western Australia, 2 June 1979 (BMR Report 1979/215)*; Bureau of Mineral Resources, Geology and Geophysics: Canberra, ACT, Australia, 1979. Available online: <http://pid.geoscience.gov.au/dataset/ga/15123> (accessed on 2 August 2019).
41. Lewis, J.D.; Daetwyler, N.A.; Bunting, J.A.; Montcrieff, J.S. *The Cadoux Earthquake (GSWA Report 11)*; Geological Survey of Western Australia: Perth, Australia, 1981.
42. Dent, V.F.; Gregson, P.J. *Cadoux Microearthquake Survey 1983 (BMR Report 1986/022)*; 1986/22; Bureau of Mineral Resources, Geology and Geophysics: Canberra, ACT, Australia, 1986. Available online: <http://pid.geoscience.gov.au/dataset/ga/14114> (accessed on 2 August 2019).
43. Denham, D.; Alexander, L.G.; Everingham, I.B.; Gregson, P.J.; McCaffrey, R.; Enever, J.R. The 1979 Cadoux earthquake and intraplate stress in Western Australia. *Aust. J. Earth Sci.* **1987**, *34*, 507–521. [CrossRef]
44. Dent, V.F. *The Distribution of Cadoux Aftershocks: Additional Results from Temporary Stations near Cadoux, 1983 (BMR Record 1988/51)*; Bureau of Mineral Resources, Geology and Geophysics: Canberra, ACT, Australia, 1988. Available online: <http://pid.geoscience.gov.au/dataset/ga/14238> (accessed on 2 August 2019).
45. Dent, V.F. Hypocentre locations from a microearthquake survey, Cadoux, Western Australia, 1983. *BMR J. Aust. Geol. Geophys.* **1991**, *12*, 1–4. Available online: <http://pid.geoscience.gov.au/dataset/ga/81278> (accessed on 2 August 2019).

46. Barlow, B.C.; Denham, D.; Jones, T.; McCue, K. The Musgrave Ranges earthquake of March 30, 1986. *Trans. R. Soc. S. Aust.* **1986**, *110*, 187–189. [[CrossRef](#)]
47. McCue, K.; Jones, T.; Michael-Leiba, M.; Barlow, B.C.; Denham, D.; Gibson, G. Another chip off the old Australian block. *Eos Trans. Am. Geophys. Union* **1987**, *68*, 609. [[CrossRef](#)]
48. Bowman, J.R.; Barlow, B.C. *Surveys of the Fault Scarp of the 1986 Marryat Creek, South Australia, Earthquake (BMR Record 1991/109)*; Australian Seismological Centre, Bureau of Mineral Resources: Canberra, ACT, Australia, 1991. Available online: <http://pid.geoscience.gov.au/dataset/ga/14490> (accessed on 2 August 2019).
49. Machette, M.N.; Crone, A.J.; Bowman, J.R.; Prescott, J.R. *Surface ruptures and deformation associated with the 1988 Tennant Creek and 1986 Marryat Creek, Australia, intraplate earthquakes. Abstracts of the U.S. Geological Survey, Central Region; 1991 Poster Review*; U.S. Geological Survey: Reston, VA, USA, 1991; p. 27. Available online: <https://doi.org/10.3133/ofr91582> (accessed on 2 August 2019).
50. Bullock, P.W.B. *Tennant Creek Gravity and Magnetic Survey, Northern Territory, 1973 (BMR Record 1977/30)*; Bureau of Mineral Resources, Geology and Geophysics: Canberra, Australia, 1977. Available online: <http://pid.geoscience.gov.au/dataset/ga/13559> (accessed on 2 August 2019).
51. Hone, I.G. *Ground Geophysical Survey, Tennant Creek, Northern Territory, 1972 (BMR Record 1974/171)*; Bureau of Mineral Resources, Geology and Geophysics: Canberra, Australia, 1974. Available online: <http://pid.geoscience.gov.au/dataset/ga/1321> (accessed on 2 August 2019).
52. Verhoeven, T.J.; Russell, P.W. *Tennant Creek Water Supply 1979 - 1980 Source Investigation [Kelly Well] (Report 27/1981)*; Department of Transport and Works: Alice Springs, Australia, 1981. Available online: <http://hdl.handle.net/10070/229202> (accessed on 2 August 2019).
53. Bowman, J.R. Constraints on locations of large intraplate earthquakes in the Northern Territory, Australia from observations at the Warramunga seismic array. *Geophys. Res. Lett.* **1988**, *15*, 1475–1478. [[CrossRef](#)]
54. Bowman, J.R.; Gibson, G.; Jones, T. Faulting process of the January 22, 1988 Tennant Creek, Northern Territory, Australia earthquakes. In *Abstracts for the AGU Fall Meeting 1988: EoS Transactions*; American Geophysical Union: Washington, USA, 1988; Volume 69, p. 1301. [[CrossRef](#)]
55. McCaffrey, R. Teleseismic investigation of the January 22, 1988 Tennant Creek, Australia, earthquakes. *Geophys. Res. Lett.* **1989**, *16*, 413–416. [[CrossRef](#)]
56. Bowman, J.R.; Dewey, J.W.; Peters, N. Recent Results from Tennant Creek. In *Recent Intraplate Seismicity Studies Symposium, Perth Western Australia (BMR Record 1990/44)*; Gregson, P.J., Ed.; Bureau of Mineral Resources, Geology and Geophysics: Canberra, ACT, Australia, 1990. Available online: <http://pid.geoscience.gov.au/dataset/ga/14335> (accessed on 2 August 2019).
57. Choy, G.L.; Bowman, J.R. Rupture process of a multiple main shock sequence: Analysis of teleseismic, local and field observations of the Tennant Creek, Australia, earthquakes of January 22, 1988. *J. Geophys. Res.* **1990**, *95*, 6867–6882. [[CrossRef](#)]
58. Bouniot, E.; Jones, T.; McCue, K. The pattern of 1987 sequence at Tennant Creek, NT. In *Recent Intraplate Seismicity Studies Symposium, Perth Western Australia (BMR Record 1990/44)*; Gregson, P.J., Ed.; Bureau of Mineral Resources, Geology and Geophysics: Canberra, ACT, Australia, 1990. Available online: <http://pid.geoscience.gov.au/dataset/ga/14335> (accessed on 2 August 2019).
59. Bowman, J.R.; Gibson, G.; Jones, T. Aftershocks of the 1988 January 22 Tennant Creek, Australia Intraplate Earthquakes: Evidence For A Complex Thrust-Fault Geometry. *Geophys. J. Int.* **1990**, *100*, 87–97. [[CrossRef](#)]
60. Jones, T.; Gibson, G.; McCue, K.; Denham, D.; Gregson, P.J.; Bowman, J.R. Three large intraplate earthquakes near Tennant Creek, Northern Territory, on 22 January 1988. *BMR J. Aust. Geol. Geophys.* **1991**, *12*, 339–343. Available online: <http://pid.geoscience.gov.au/dataset/ga/81300> (accessed on 2 August 2019).
61. Bowman, J.R.; Dewey, J.W. Relocation of teleseismically recorded earthquakes near Tennant Creek, Australia: Implications for midplate seismogenesis. *J. Geophys. Res.* **1991**, *96*, 11973–11979. [[CrossRef](#)]
62. Bowman, J.R. Geodetic evidence for conjugate faulting during the 1988 Tennant Creek, Australia earthquake sequence. *Geophys. J. Int.* **1991**, *107*, 47–56. [[CrossRef](#)]
63. Crone, A.J.; Machette, M.N.; Bowman, J.R. *Geologic Investigations of the 1988 Tennant Creek, Australia, Earthquakes - Implications for Paleoseismicity in the Stable Continental Regions (USGS Bulletin 2032-A)*; U.S. Geological Survey: Washington, DC, USA, 1992.
64. Bowman, J.R. The 1988 Tennant Creek, Northern Territory, earthquakes: A synthesis. *Aust. J. Earth Sci.* **1992**, *39*, 651–669. [[CrossRef](#)]

65. Donnelly, K.E.; Morrison, R.S.; Hussey, K.J.; Ferenczi, P.A.; Kruse, P.D. *Tennant Creek 1:250000 Explanatory Notes, Geological Map Series*; Northern Territory Geological Survey: Darwin, Australia, 1999. Available online: <https://doi.org/10.1017/CBO9781107415324.004> (accessed on 2 August 2019).
66. Johnstone, A.; Donnellan, N. *Tennant Creek 1:250 000 Integrated Interpretation of Geophysics and Mapped Geology*, 1st ed.; Northern Territory Geological Survey, Alice Springs: Alice Springs, Australia, 2001.
67. Bowman, J.R.; Yong, C. Case 22 A Seismicity Precursor to a Sequence of M 6.3–6.7 Midplate Earthquakes in Australia. *Pure Appl. Geophys.* **1997**, *149*, 61–78. [[CrossRef](#)]
68. Donnellan, N. Chapter 9: Warramunga Province. In *Geology and Mineral Resources of the Northern Territory, Special Publication 5*; Ahmad, M., Munson, T.J., Eds.; Special Pu. Northern Territory Geological Survey: Darwin, Australia, 2013.
69. Mohammadi, H.; Quigley, M.; Steacy, S.; Duffy, B. Effects of source model variations on Coulomb stress analyses of a multi-fault intraplate earthquake sequence. *Tectonophysics* **2019**, *766*, 151–166. [[CrossRef](#)]
70. Dawson, J.; Cummins, P.R.; Tregoning, P.; Leonard, M. Shallow intraplate earthquakes in Western Australia observed by Interferometric Synthetic Aperture Radar. *J. Geophys. Res. Solid Earth* **2008**, *113*, 1–19. [[CrossRef](#)]
71. Dent, V.F. Improved Hypocentral estimates for two recent seismic events in south-western Western Australia, using temporary station data. In Proceedings of the Australian Earthquake Engineering Society Conference 2008, Ballarat, VIC, Australia, 21–23 November 2008.
72. Clark, D.; McPherson, A. A tale of two seisms: Ernabella 23/03/2012 (Mw5.4) and Mulga Park 09/06/2013 (Mw 5.6). *Aust. Earthq. Eng. Soc. Newsl.* **2013**, *2013*, 7–11.
73. King, T.R.; Quigley, M.C.; Clark, D. Earthquake environmental effects produced by the Mw 6.1, 20th May 2016 Petermann earthquake, Australia. *Tectonophysics* **2018**, *747–748*, 357–372. [[CrossRef](#)]
74. Hejrani, B.; Tkalčić, H. The 20 May 2016 Petermann Ranges earthquake: Centroid location, magnitude and focal mechanism from full waveform modelling. *Aust. J. Earth Sci.* **2018**, *66*, 37–45. [[CrossRef](#)]
75. Polcari, M.; Albano, M.; Atzori, S.; Bignami, C.; Stramondo, S.; Polcari, M.; Albano, M.; Atzori, S.; Bignami, C.; Stramondo, S. The Causative Fault of the 2016 Mw 6.1 Petermann Ranges Intraplate Earthquake (Central Australia) Retrieved by C- and L-Band InSAR Data. *Remote Sens.* **2018**, *10*, 1311. [[CrossRef](#)]
76. Wang, S.; Xu, W.; Xu, C.; Yin, Z.; Bürgmann, R.; Liu, L.; Jiang, G. Changes in groundwater level possibly encourage shallow earthquakes in central Australia: The 2016 Petermann Ranges earthquake. *Geophys. Res. Lett.* **2019**, *46*, 3189–3198. [[CrossRef](#)]
77. Gold, R.; Clark, D.; King, T.; Quigley, M. *Surface rupture and vertical deformation associated with 20 May 2016 M6 Petermann Ranges earthquake, Northern Territory, Australia*; European Geosciences Union General Assembly: Vienna, Austria, 2017; Volume 19. Available online: <http://adsabs.harvard.edu/abs/2017EGUGA..19.8645G> (accessed on 2 August 2019).
78. Gold, R.D.; Clark, D.; Barnhart, W.D.; King, T.; Quigley, M.; Briggs, R.W. Surface rupture and distributed deformation revealed by optical satellite imagery: The intraplate 2016 Mw 6.0 Petermann Ranges earthquake, Australia. *Geophys. Res. Lett.* **2019**. [[CrossRef](#)]
79. Clark, D.J.; Brennand, S.; Brenn, G.; Allen, T.I.; Garthwaite, M.C.; Standen, S. The 2018 Lake Muir earthquake sequence, southwest Western Australia: Rethinking Australian stable continental region earthquakes. *Solid Earth* **2019**. in review. [[CrossRef](#)]
80. Doyle, H.A.; Everingham, I.B.; Sutton, D.J. Seismicity of the Australian continent. *J. Geol. Soc. Aust.* **1968**, *15*, 295–312. [[CrossRef](#)]
81. Cleary, J.R.; Simpson, D.W. Seismotectonics of the Australian continent. *Nature* **1971**, *230*, 239–241. [[CrossRef](#)]
82. Doyle, H.A. Seismicity and structure in Australia. *Bull. R. Soc. N. Z.* **1971**, *9*, 149–152.
83. Denham, D.; Alexander, L.G.; Worotnicki, G. Stresses in the Australian crust: Evidence from earthquakes and in-situ stress measurements. *BMR J. Aust. Geol. Geophys.* **1979**, *4*, 289–295. Available online: <http://pid.geoscience.gov.au/dataset/ga/81007> (accessed on 2 August 2019).
84. Everingham, I.B.; McEwin, A.J.; Denham, D. *Atlas of Isoseismal Maps of Australian Earthquakes*; Bureau of Mineral Resources, Geology and Geophysics: Canberra, Australia, 1982. Available online: <http://pid.geoscience.gov.au/dataset/ga/38> (accessed on 2 August 2019).
85. Lambeck, K.; McQueen, H.W.S.; Stephenson, R.A.; Denham, D. The state of stress within the Australian continent. *Ann. Geophys.* **1984**, *2*, 723–742.

86. Rynn, J.M.W.; Denham, D.; Greenhalgh, S.A.; Jones, T.; Gregson, P.J.; McCue, K.; Smith, R.S. *Atlas of Iseismal Maps of Australian Earthquakes, Part 2*; Bureau of Mineral Resources, Geology and Geophysics: Canberra, ACT, Australia, 1987. Available online: <http://pid.geoscience.gov.au/dataset/ga/19> (accessed on 2 August 2019).
87. Johnston, A. Fault Traces Australian Quakes. *Eos Trans. Am. Geophys. Union* **1988**, *69*, 682. [[CrossRef](#)]
88. Denham, D. Australian seismicity—the puzzle of the not-so-stable continent. *Seismol. Res. Lett.* **1988**, *59*, 235–240. [[CrossRef](#)]
89. McCue, K. Australia's large earthquakes and Recent fault scarps. *J. Struct. Geol.* **1990**, *12*, 761–766. [[CrossRef](#)]
90. Leonard, M.; Ripper, I.D.; Yue, L. *Australian Earthquake Fault Plane Solutions (GA Record 2002/019)*; 2002/19; Geoscience Australia: Canberra, ACT, Australia, 2002. Available online: <http://pid.geoscience.gov.au/dataset/ga/37302> (accessed on 2 August 2019).
91. Dentith, M.; Featherstone, W.E. Controls on intra-plate seismicity in southwestern Australia. *Tectonophysics* **2003**, *376*, 167–184. [[CrossRef](#)]
92. Featherstone, W.E.; Penna, T. N.; Leonard, M.; Clark, D.; Dawson, J.; Dentith, M.; Darby, D.; McCarthy, R. GPS-geodetic deformation monitoring of the south-west seismic zone of Western Australia: Review, description of methodology and results from epoch-one. *J. R. Soc. West Aust.* **2004**, *87*, 1–8.
93. Dawson, J.; Tregoning, P. Uncertainty analysis of earthquake source parameters determined from InSAR: A simulation study. *J. Geophys. Res. Solid Earth* **2007**, *112*, 1–13. [[CrossRef](#)]
94. Braun, J.; Burbidge, D.R.; Gesto, F.N.; Sandiford, M.; Gleadow, A.J.W.; Kohn, B.P.; Cummins, P.R. Constraints on the current rate of deformation and surface uplift of the Australian continent from a new seismic database and low-T thermochronological data. *Aust. J. Earth Sci.* **2009**, *56*, 99–110. [[CrossRef](#)]
95. Clark, D. *Neotectonic Features Database*; Geoscience Australia, Commonwealth of Australia: Canberra, Australia, 2012.
96. Clark, D.; Allen, T. What have we learnt regarding cratonic earthquakes in the fifty years since Meckering? In Proceedings of the Australian Earthquake Engineering Society Conference 2018, Perth, WA, USA, 16–18 November 2018.
97. Tracey, R.M. Analysis of Repeat Levelling Measurements to Give Ground Deformation, Southwest Australia (BMR Record 1982/30). Bureau of Mineral Resources, Geology and Geophysics: Canberra, Australia, 1982.
98. Dent, V.F. *Hypocentre Relocations Using Data from Temporary Seismograph Stations at Burakin and Wyalkatchem, Western Australia (BMR Record 1990/36)*; Bureau of Mineral Resources, Geology and Geophysics: Canberra, Australia, 1990. Available online: <http://pid.geoscience.gov.au/dataset/ga/14327> (accessed on 2 August 2019).
99. Leonard, M.; Burbidge, D.R.; Allen, T.; Robinson, D.J.; Mcpherson, A.; Clark, D.; Collins, C. The challenges of probabilistic seismic-hazard assessment in stable continental interiors: An Australian example. *Bull. Seismol. Soc. Am.* **2014**, *104*, 3008–3028. [[CrossRef](#)]
100. Rajabi, M.; Tingay, M.; Heidbach, O.; Hillis, R.R.; Reynolds, S.D. The present-day stress field of Australia. *Earth-Sci. Rev.* **2017**, *168*, 165–189. [[CrossRef](#)]
101. Hillis, R.R.; Sandiford, M.; Reynolds, S.D.; Quigley, M.C. Present-day stresses, seismicity and Neogene-to-Recent tectonics of Australia's "passive" margins: Intraplate deformation controlled by plate boundary forces. *Geol. Soc. Lond. Spec. Publ.* **2008**, *306*, 71–90. [[CrossRef](#)]
102. Leonard, M. One hundred years of earthquake recording in Australia. *Bull. Seismol. Soc. Am.* **2008**, *98*, 1458–1470. [[CrossRef](#)]
103. Raymond, O.L.; Totterdell, J.M.; Stewart, A.J.; Woods, M.A. *Australian Geological Provinces: 2018.01 Edition [Digital Dataset]*; Geoscience Australia, Commonwealth of Australia: Canberra, Australia, 2018. Available online: <http://pid.geoscience.gov.au/dataset/ga/116823> (accessed on 2 August 2019).
104. Johnston, A.C.; Coppersmith, K.J.; Cornell, C.A. The earthquakes of stable continental regions. In *Electric Power Research Institute Report TR-102261-VI*; EPRI Distribution Centre: Palo Alto, CA, USA, 1994.
105. Rajabi, M.; Heidbach, O.; Tingay, M.; Reiter, K. Prediction of the present-day stress field in the Australian continental crust using 3D geomechanical–numerical models. *Aust. J. Earth Sci.* **2017**, *64*, 435–454. [[CrossRef](#)]
106. Clark, D. Identification of quaternary scarps in southwest and central west Western Australia using dem-based hill shading: Application to seismic hazard assessment and neotectonics. *Int. J. Remote Sens.* **2010**, *31*, 6297–6325. [[CrossRef](#)]

107. Clark, D.; Cupper, M.; Sandiford, M.; Kiernan, K. Style and timing of late Quaternary faulting on the Lake Edgar fault, southwest Tasmania, Australia: Implications for hazard assessment in intracratonic areas. In *Geological Criteria for Evaluating Seismicity Revisited: Forty Years of Paleoseismic Investigations and the Natural Record of Past Earthquakes: Geological Society of America Special Paper 479*; Audemard, F.A., Michetti, A.M., McCalpin, J.P., Eds.; The Geological Society of America: Boulder, CO, USA, 2011; Volume 2479, pp. 109–131. [[CrossRef](#)]
108. Clark, D.; Dentith, M.; Wyrwoll, K.-H.; Yanchou, L.; Dent, V.F.; Featherstone, W.E. The Hyden fault scarp, Western Australia: Paleoseismic evidence for repeated Quaternary displacement in an intracratonic setting. *Aust. J. Earth Sci.* **2008**, *55*, 379–395. [[CrossRef](#)]
109. Quigley, M.C.; Sandiford, M.; Fifield, L.K.; Alimanovic, A. Landscape responses to intraplate tectonism: Quantitative constraints from ¹⁰Be nuclide abundances. *Earth Planet Sci. Lett.* **2007**, *261*, 120–133. [[CrossRef](#)]
110. Quigley, M.C.; Sandiford, M.; Cupper, M. Distinguishing tectonic from climatic controls on range-front sedimentation. *Basin Res.* **2007**, *19*, 491–505. [[CrossRef](#)]
111. Quigley, M.C.; Cupper, M.; Sandiford, M. Quaternary faults of south-central Australia: Palaeoseismicity, slip rates and origin. *Aust. J. Earth Sci.* **2006**, *53*, 285–301. [[CrossRef](#)]
112. Thom, R. A recent fault scarp in the Lort River area, Ravensthorpe 1:250 000 sheet. In *Geological Survey of Western Australia Annual Report 1971*; Geological Survey of Western Australia: Perth, Australia, 1971; pp. 58–59.
113. Williams, I.R. Recent fault scarps in the Mount Narryer area, byro 1:250 000 sheet. In *Geological Survey of Western Australia Annual Report 1978*; Geological Survey of Western Australia: Perth, Australia, 1978.
114. Wilde, S.A.; Low, G.H.; Lake, R.W. *Perth 1:250 000 Geological Map Sheet*; Geological Survey of Western Australia: Perth, Western Australia, 1978.
115. Blight, D.F.; Chin, R.J.; Smith, R.A.; Bunting, J.A.; Elias, M. *Bencubbin 1:250 000 Geological Map Sheet*; Geological Survey of Western Australia: Perth, Australia, 1983.
116. Scrimgeour, I.R.; Close, D.F.; Edgoose, C.J. *Petermann Ranges SG52-7; Explanatory Notes*; Northern Territory Geological Survey: Darwin, Australia, 1999.
117. Fairclough, M.C.; Sprigg, R.C.; Wilson, B.; Coats, R.P. *Alberga 1:250 000 Geological Map, Digital Edition*; Geological Survey of South Australia: Adelaide, Australia, 2011.
118. Machette, M.N.; Crone, A.J.; Bowman, J.R. *Geologic Investigations of the 1986 Marryat Creek, Australia, Earthquake: Implications for Paleoseismicity in Stable Continental Regions (USGS Bulletin 2032-B)*; U.S. Geological Survey: Washington, DC, USA, 1993. [[CrossRef](#)]
119. Allen, T.; Griffin, J.; Leonard, M.; Clark, D.; Ghasemi, H. *The 2018 National Seismic Hazard Assessment: Model Overview (GA Record 2018/27)*; Geoscience Australia, Commonwealth of Australia: Canberra, Australia, 2018.
120. King, T.R.; Quigley, M.; Clark, D. Review paper: The 14th October 1968 Mw 6.6 Meckering surface rupturing earthquake, Australia. *EarthArXiv Prepr.* **2019**, 1–25. [[CrossRef](#)]
121. King, T.R.; Quigley, M.C.; Clark, D. Review paper: The 10th March 1970 Mw 5.0 Calingiri surface rupturing earthquake, Australia. *EarthArXiv Prepr.* **2019**. [[CrossRef](#)]
122. King, T.R.; Quigley, M.C.; Clark, D. Review paper: The 2nd June 1979 Mw 6.1 Cadoux surface rupturing earthquake, Australia. *EarthArXiv Prepr.* **2019**, 1–19. [[CrossRef](#)]
123. King, T.R.; Quigley, M.C.; Clark, D. Review paper: The 30th March 1968 Mw 5.7 Marryat Creek surface rupturing earthquake, Australia. *EarthArXiv Prepr.* **2019**, 1–17. [[CrossRef](#)]
124. King, T.R.; Quigley, M.; Clark, D. Review paper: The 23rd March 2012 Mw 5.2 Pukatja surface rupturing earthquake, Australia. *EarthArXiv Prepr.* **2019**, 1–13. [[CrossRef](#)]
125. King, T.R.; Quigley, M.; Clark, D. Review paper: The 20th May 2016 Mw 6.1 Petermann surface rupturing earthquake, Australia. *EarthArXiv Prepr.* **2019**, 1–16. [[CrossRef](#)]
126. King, T.R.; Quigley, M.C.; Clark, D.; Valkaniotis, S.; Mohammadi, H.; Barnhart, W.D. The 1987 to 2019 Tennant Creek, Australia, earthquake sequence: A protracted intraplate multi-mainshock sequence. *EarthArXiv Prepr.* **2019**. [[CrossRef](#)]
127. Wilde, S.A.; Middleton, M.F.; Evans, B.J. Terrane accretion in the southwestern Yilgarn Craton: Evidence from a deep seismic crustal profile. *Precambrian Res.* **1996**, *78*, 179–196. [[CrossRef](#)]
128. Edgoose, C.J.; Scrimgeour, I.R.; Close, D.F. *Geology of the Musgrave Block, Northern Territory (NTGS Report 15)*; Munson, T.J., Ed.; Northern Territory Geological Survey: Darwin, Australia, 2004.

129. Raimondo, T.; Collins, A.S.; Hand, M.; Walker-Hallam, A.; Smithies, R.H.; Evins, P.M.; Howard, H.M. The anatomy of a deep intracontinental orogen. *Tectonics* **2010**, *29*. [[CrossRef](#)]
130. Neumann, N.L. (Ed.) *Yilgarn Craton – Officer Basin – Musgrave Province Seismic and MT Workshop (GA Record 2013/28)*; Geoscience Australia, Commonwealth of Australia: Canberra, ACT, Australia, 2013. Available online: <http://pid.geoscience.gov.au/dataset/ga/76664> (accessed on 2 August 2019).
131. Wade, B.P.; Kelsey, D.E.; Hand, M.; Barovich, K.M. The Musgrave Province: Stitching north, west and south Australia. *Precambrian Res.* **2008**, *166*, 370–386. [[CrossRef](#)]
132. Donnellan, N.; Hussey, K.J.; Morrisson, R.S.; Kruse, P.D. *Tennant Creek 1:250 000 Geology*, 2nd ed.; Northern Territory Geological Survey: Darwin, Australia, 1998.
133. Brakel, A.T.; Montcrieff, J.S.; Muhling, P.D.; Chin, R.J. *Dumbleyung 1:250 000 Geological Map*; Geological Survey of Western Australia: Perth, Australia, 1985.
134. Scrimgeour, I.R.; Close, D.F.; Edgoose, C.J. *Petermann Ranges 1:250 000 Geological Map*, 2nd ed.; Northern Territory Geological Survey: Darwin, Australia, 1999.
135. Quigley, M.C.; Mohammadi, H.; Jimenez, A.; Duffy, B.G. Multi-fault earthquakes with kinematic and geometric rupture complexity: How common? INQUA Focus Group Earthquake Geology and Seismic Hazards. In Proceedings of the 8th International INQUA Meeting on Paleoseismology, Active Tectonics and Archeoseismology (PATA), Blenheim, New Zealand, 13–16 November 2017.
136. Bowman, J.R.; Jones, T. *Post-Seismic Surveys of the Epicentral Area of the 1988 Tennant Creek, N.T., Earthquakes (BMR Record 1992/002)*; Bureau of Mineral Resources, Geology and Geophysics: Canberra, Australia, 1991. Available online: <http://pid.geoscience.gov.au/dataset/ga/14510> (accessed on 2 August 2019).
137. Rogers, C.D.F. Types and distribution of collapsible soils. In *Genesis and Properties of Collapsible Soils*; Derbyshire, E., Dijkstra, T., Smalley, I.J., Eds.; Springer: Loughborough, UK, 1995; pp. 1–17.
138. Bierman, P.R.; Caffee, M.W. Cosmogenic exposure and erosion history of Australian bedrock landforms. *Bull. Geol. Soc. Am.* **2002**, *114*, 787–803. [[CrossRef](#)]
139. Biasi, G.P.; Wesnousky, S.G. Bends and ends of surface ruptures. *Bull. Seismol. Soc. Am.* **2017**, *107*, 2543–2560. [[CrossRef](#)]
140. Mcpherson, A.; Clark, D.; Macphail, M.; Cupper, M. Episodic post-rift deformation in the south-eastern Australian passive margin: Evidence from the Lapstone Structural Complex. *Earth Surf. Process. Landf.* **2014**, *39*, 1449–1466. [[CrossRef](#)]
141. Allen, T.; Griffin, J.; Clark, D. *The 2018 National Seismic Hazard Assessment: Model Input Files (GA Record 2018/032)*; 2018/32; Geoscience Australia: Canberra, ACT, Australia, 2018. [[CrossRef](#)]
142. Clark, D.; Leonard, M.; Griffin, J.; Stirling, M.W.; Volti, T. Incorporating fault sources into the Australian National Seismic Hazard Assessment (NSHA) 2018. In Proceedings of the Australian Earthquake Engineering Society Conference 2016, Melbourne, VIC, Australia, 25–27 November 2016.
143. Boncio, P.; Liberi, F.; Caldarella, M.; Nurminen, F.C. Width of surface rupture zone for thrust earthquakes: Implications for earthquake fault zoning. *Nat. Hazards Earth Syst. Sci.* **2018**, *18*, 241–256. [[CrossRef](#)]
144. Leonard, M. Earthquake fault scaling: Self-consistent relating of rupture length, width, average displacement, and moment release. *Bull. Seismol. Soc. Am.* **2010**, *100*, 1971–1988. [[CrossRef](#)]
145. Moss, R.E.S.; Ross, Z.E. Probabilistic fault displacement hazard analysis for reverse faults. *Bull. Seismol. Soc. Am.* **2011**, *101*, 1542–1553. [[CrossRef](#)]
146. Lavrentiadis, G.; Abrahamson, N. Generation of surface-slip profiles in the wavenumber domain. *Bull. Seismol. Soc. Am.* **2019**, *109*, 888–907. [[CrossRef](#)]
147. Anderson, J.G.; Biasi, G.P.; Wesnousky, S.G. Fault-scaling relationships depend on the average fault-slip rate. *Bull. Seismol. Soc. Am.* **2017**, *107*, 2561–2577. [[CrossRef](#)]
148. Leonard, M. Self-consistent earthquake fault-scaling relations: Update and extension to stable continental strike-slip faults. *Bull. Seismol. Soc. Am.* **2014**, *104*, 2953–2965. [[CrossRef](#)]
149. Finch, E.; Hardy, S.; Gawthorpe, R. Discrete-element modelling of contractional fault-propagation folding above rigid basement fault blocks. *J. Struct. Geol.* **2003**, *25*, 515–528. [[CrossRef](#)]
150. Serva, L. History of the Environmental Seismic Intensity Scale ESI-07. *Geosciences* **2019**, *9*, 210. [[CrossRef](#)]
151. Ahmad, B.; Sana, H.; Alam, A. Macroseismic intensity assessment of 1885 Baramulla Earthquake of northwestern Kashmir Himalaya, using the Environmental Seismic Intensity scale (ESI 2007). *Quat. Int.* **2014**, *321*, 59–64. [[CrossRef](#)]

152. Sanchez, J.J.; Maldonado, R.F. Application of the ESI 2007 scale to two large earthquakes: South Island, New Zealand (2010 Mw 7.1), and Tohoku, Japan (2011 Mw 9.0). *Bull. Seismol. Soc. Am.* **2016**, *106*, 1151–1161. [[CrossRef](#)]
153. Nappi, R.; Gaudiosi, G.; Alessio, G.; De Lucia, M.; Porfido, S. The environmental effects of the 1743 Salento earthquake (Apulia, southern Italy): A contribution to seismic hazard assessment of the Salento Peninsula. *Nat. Hazards* **2017**, *86*, S295–S324. [[CrossRef](#)]
154. Serva, L.; Vittori, E.; Commerci, V.; Esposito, E.; Guerrieri, L.; Michetti, A.M.; Mohammadioun, B.; Mohammadioun, G.C.; Porfido, S.; Tatevossian, R.E. Earthquake Hazard and the Environmental Seismic Intensity (ESI) Scale. *Pure Appl. Geophys.* **2016**, *173*, 1479–1515. [[CrossRef](#)]
155. Mitchell, D.; Paultre, P.; Tinawi, R.; Saatcioglu, M.; Tremblay, R.; Elwood, K.; Adams, J.; DeVall, R. Earthquake Environmental Effect for seismic hazard assessment: The ESI intensity scale and the EEE Catalogue. *Mem Descr della Cart Geol d'Italia* **2015**, *97*, 1–181.
156. Porfido, S.; Esposito, E.; Spiga, E.; Sacchi, M.; Molisso, F.; Mazzola, S. Impact of Ground Effects for an Appropriate Mitigation Strategy in Seismic Area: The Example of Guatemala 1976 Earthquake. In *Engineering Geology for Society and Territory - Volume 2: Landslide Processes*; Lollino, G., Giordan, D., Crosta, G.B., Corominas, J., Azzam, R., Wasowski, J., Sciarra, N., Eds.; Springer International Publishing: Berlin, Germany, 2015; pp. 703–708. [[CrossRef](#)]
157. Reicherter, K.; Michetti, A.M.; Silva, P.G.; Silva Barroso, P.G. Palaeoseismology: Historical and prehistorical records of earthquake ground effects for seismic hazard assessment. *Geol. Soc. Lond. Spec. Publ.* **2009**, *316*, 1–10. [[CrossRef](#)]
158. Giner-Robles, J.L.; Silva, P.G.; Elez, J.; Rodríguez-Pascua, M.A.; Perez-Lopez, R.; Rodríguez-Escudero, E. Relationships between the ESI-07 scale and expected PGA values from the analysis of two historical earthquakes (\geq VIII EMS) in East Spain: Tavernes 1396 AD and Estubeny 1748 AD events. In Proceedings of the 6th International INQUA Meeting in Paleoseismology, Active Tectonics and Archaeoseismology, Pescina, Fucino Basin, Italy, 19–24 April 2015.
159. Heddar, A.; Beldjoudi, H.; Aurhemayou, C.; SiBachir, R.; Yelles-Chaouche, A.; Boudiaf, A. Use of the ESI-2007 scale to evaluate the 2003 Boumerdès earthquake (North Algeria). *Ann. Geophys.* **2016**, *5*. [[CrossRef](#)]
160. Johnston, A.C. Seismotectonic interpretations and conclusions from the stable continental region seismicity database. In *The Earthquakes of Stable Continental Regions—v. 1 Assessment of Large Earthquake Potential*; Johnston, A.C., Coppersmith, K.J., Kanter, L.R., Cornell, C.A., Eds.; Electric Power Research Institute: Palo Alto, CA, USA, 1994.
161. Griffin, J.; Weatherill, G.; Allen, T. Performance of national scale smoothed seismicity estimates of earthquake activity rates. In Proceedings of the Australian Earthquake Engineering Society 2017 Conference, Canberra, ACT, Australia, 24–26 November 2017.
162. Adams, J.; Percival, J.A.; Wetmiller, R.J.; Drysdale, J.A.; Robertson, P.B. Geological controls on the 1989 Ungava surface rupture: A preliminary interpretation (GSC Paper 92-1C). In *Current Research, Part C*; Geological Survey of Canada: Ottawa, ON, Canada, 1992; pp. 147–155. [[CrossRef](#)]
163. Bent, A.L. The 1989 (Ms 6.3) Ungava, Quebec, Earthquake: A Complex Intraplate Event. *Bull. Seismol. Soc. Am.* **1994**, *84*, 1075–1088.
164. Mitchell, D.; Paultre, P.; Tinawi, R.; Saatcioglu, M.; Tremblay, R.; Elwood, K.; Adams, J.; DeVall, R. Evolution of seismic design provisions in the National building code of Canada. *Can. J. Civ. Eng.* **2010**, *37*, 1157–1170. [[CrossRef](#)]
165. Beekman, F.; Stephenson, R.A.; Korsch, R.J. Mechanical stability of the Redbank Thrust Zone, Central Australia: Dynamic and rheological implications. *Aust. J. Earth Sci.* **1997**, *44*, 215–226. [[CrossRef](#)]
166. Sandiford, M.; Egholm, D.L. Enhanced intraplate seismicity along continental margins: Some causes and consequences. *Tectonophysics* **2008**, *457*, 197–208. [[CrossRef](#)]
167. Everingham, I.B.; Smith, R.S. Implications of fault-plane solutions for Australian earthquakes on 4 July 1977, 6 May 1978 and 25 November 1978. *BMR J. Aust. Geol. Geophys.* **1979**, *4*, 297–301. Available online: <http://pid.geoscience.gov.au/dataset/ga/81008> (accessed on 2 August 2019).

